APPENDIX F
ARTIFICIAL NEURAL NETWORK MODELS OF STRESS INTENSITY FACTORS

TABLE OF CONTENTS

LIST OF FIGURES

LIST OF FIGURES (Continued)

LIST OF FIGURES (Continued)

LIST OF TABLES

LIST OF TABLES (Continued)

Artificial Neural Network (ANN) algorithms, while being computationally powerful, have limitations just as do regression models. One of the limitations that the two methods have in common is that they are not expected to extrapolate well beyond their inference space. Consequently, it is important for the user to be conversant with the ranges of variables upon which each of the 18 ANN algorithms used in the reflection cracking program is based. This appendix presents the ranges of the variables and the pavement structure geometries that are incorporated in each of the ANN models. It also gives the details of the degree of fit that were achieved with the computed stress intensity factors that were generated by the finite element program detailed in Appendix Q.

Three types of ANN algorithms were assembled: thermal, shear, and bending. Two types of pavement overlay structure were considered: asphalt overlays over a cracked asphalt surface layer and over jointed concrete. Some special cases were included such as asphalt overlays over continuous reinforced concrete, asphalt overlays over seal coats or open graded friction courses, and asphalt overlays with reinforcing interlayers. In the discussion that follows, the thermal cases will be presented first and then the traffic loading cases of shearing and bending. A schematic diagram of the 18 ANN algorithms is shown in Figure F-1.

The three thermal stress intensity factor interlayer models are for different levels of reinforcing stiffness which are designated as being “High”, “Medium”, and “Low”. As is explained in Chapter 2, the user may select which of these descriptions characterize a given reinforcing interlayer by referring to a chart which may be used for either grid-type or sheet type interlayers. With the grid-type, the reinforcing stiffness, S , is given by

$$S=\frac{Ea}{s} \qquad \text{(F-1)}$$

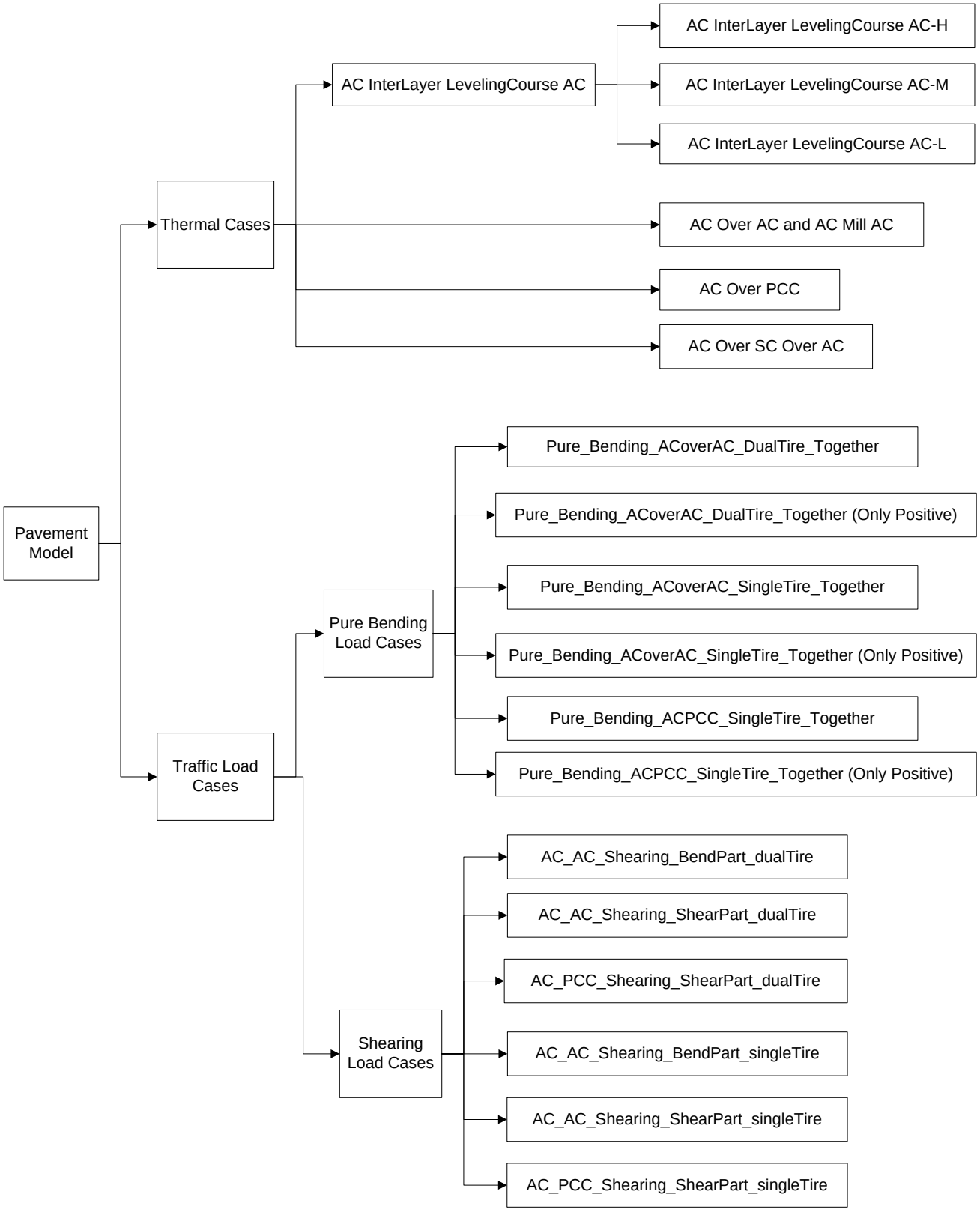

Figure F-1. Artificial neural network models for stress intensity factors.

where

S = the interlayer stiffness, MN-mm/m^2

E = the secant modulus of the grid material in the longitudinal direction, MN/m^2

a = the cross-sectional area of a rib of the grid, mm^2

s = the spacing of the ribs, mm

With a sheet-type of reinforcing interlayer, the reinforcing stiffness is given by

$$S=Et \qquad \text{(F-2)}$$

where, as before,

E = the secant modulus of the sheet material, MN/m^2

and t = the thickness of the sheet, mm

The reinforcing interlayer must be locked in to the overlay in order to reinforce it. With a grid-type of interlayer, this means that there is a sufficiently large grid opening that the largest aggregate from both above and below the interlayer can interpenetrate and lock the grid in place. An interlayer that is not locked into the mixture both above and below it does not reinforce.

The graph which may be used to select the appropriate level of reinforcing stiffness is given below in Figure F-2.

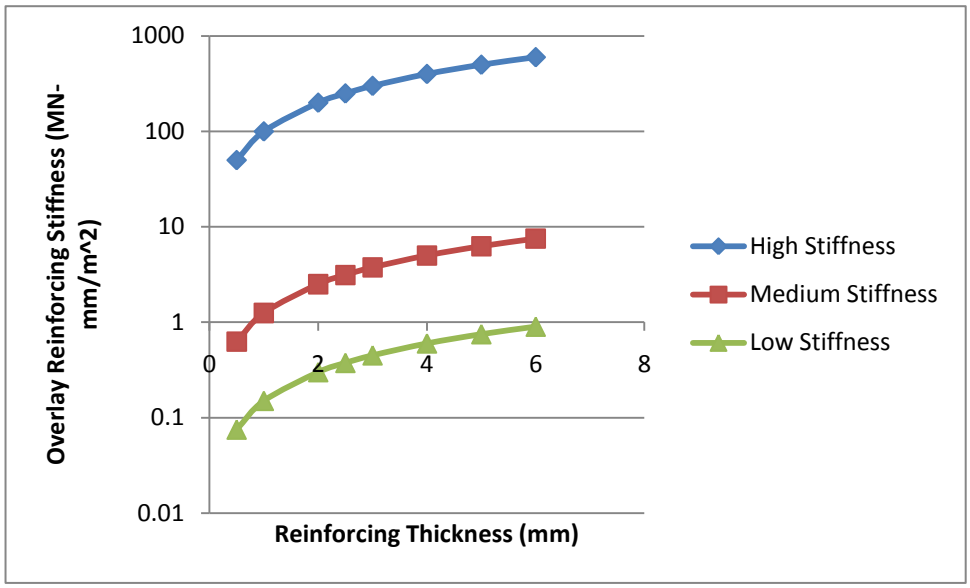

Figure F-2. Interlayer reinforcing stiffness (MN-mm/m$^{2)}$ versus reinforcing thickness (mm).

The user will plot the interlayer stiffness and thickness of the selected material on the above graph and input the stiffness description that is closest to the plotted point.

There are three bending stress intensity factor models that are described as "Only Positive" and these are the only ones that are used in calculating the bending stress intensity factors in the reflection cracking program. The "Only Positive" description refers to the fact that bending causes a reflection crack to grow only when the bending stress at the tip of the crack is tensile (or "positive"). Many of the runs of the finite element program found that the calculated bending stress at the tip of the crack was compressive and therefore, according to the sign convention, "negative." The bending stress is positive only when the crack is in the bottom of the overlay. The other three bending stress intensity factor models predict the complete set of both tensile and compressive stress intensity factors.

The thermal reflection cracking cases are illustrated in Figures F-3 through F-12. Each of these includes a sketch of the pavement structure with a list of the variables in the companion Tables F-1 through F-4 that were included in the full factorial set of finite element runs. These finite element runs generated the set of stress intensity factors that are predicted by the Artificial Neural Network algorithm.

THERMAL REFLECTION CRACKING CASES

1. HMA Overlay on Asphalt Concrete Pavement

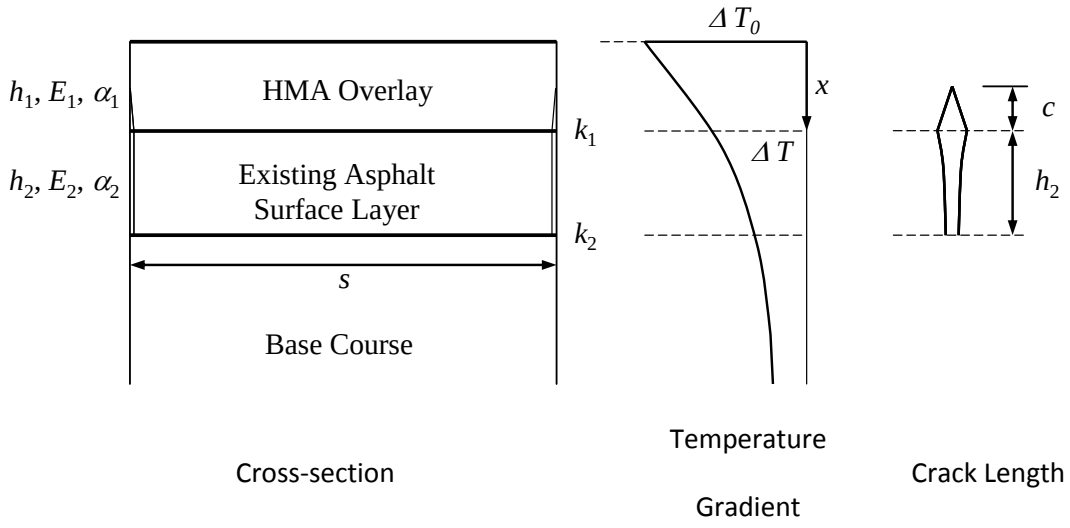

Figure F-3. Diagrams of HMA overlay on asphalt concrete pavement-thermal.

Table F-1. Thermal stress variables in HMA overlay on asphalt concrete pavement system.

Variable		Unit	Value
Overlay Layer	Thickness (h_1)	mm	38, 75, 150
	Modulus (E_1)	MPa	70, 300, 700
	Coefficient of Thermal Expansion (α_1)	strain/°C	2×10^{-5}, 4×10^{-5}
Interface Condition (k_1)*		-	1.0
Existing Surface	Thickness (h_2)	mm	100, 200, 300
	Modulus (E_2)	MPa	70, 300, 700
	Coefficient of Thermal Expansion (α_2)	strain/°C	2×10^{-5}, 4×10^{-5}
Interface Condition (k_2)*		-	1.0
Temperature Differential (ΔT_0)		°C	30
Half Crack Spacing (s/2)		mm	4500
Ratio of Crack Length to Layer Thickness (c / h_1)		-	0.1, 0.3, 0.5, 0.7, 0.9

* 0 (fully slipped) < k_i < 1.0 (fully bonded)

The Artificial Neural Network Model that was developed for the case of a thermal stress intensity factor in an asphalt overlay over an existing cracked asphalt surface layer is shown in Figure F-4. The fit that was achieved with the ANN model that was developed for this case is shown in the legend of that figure.

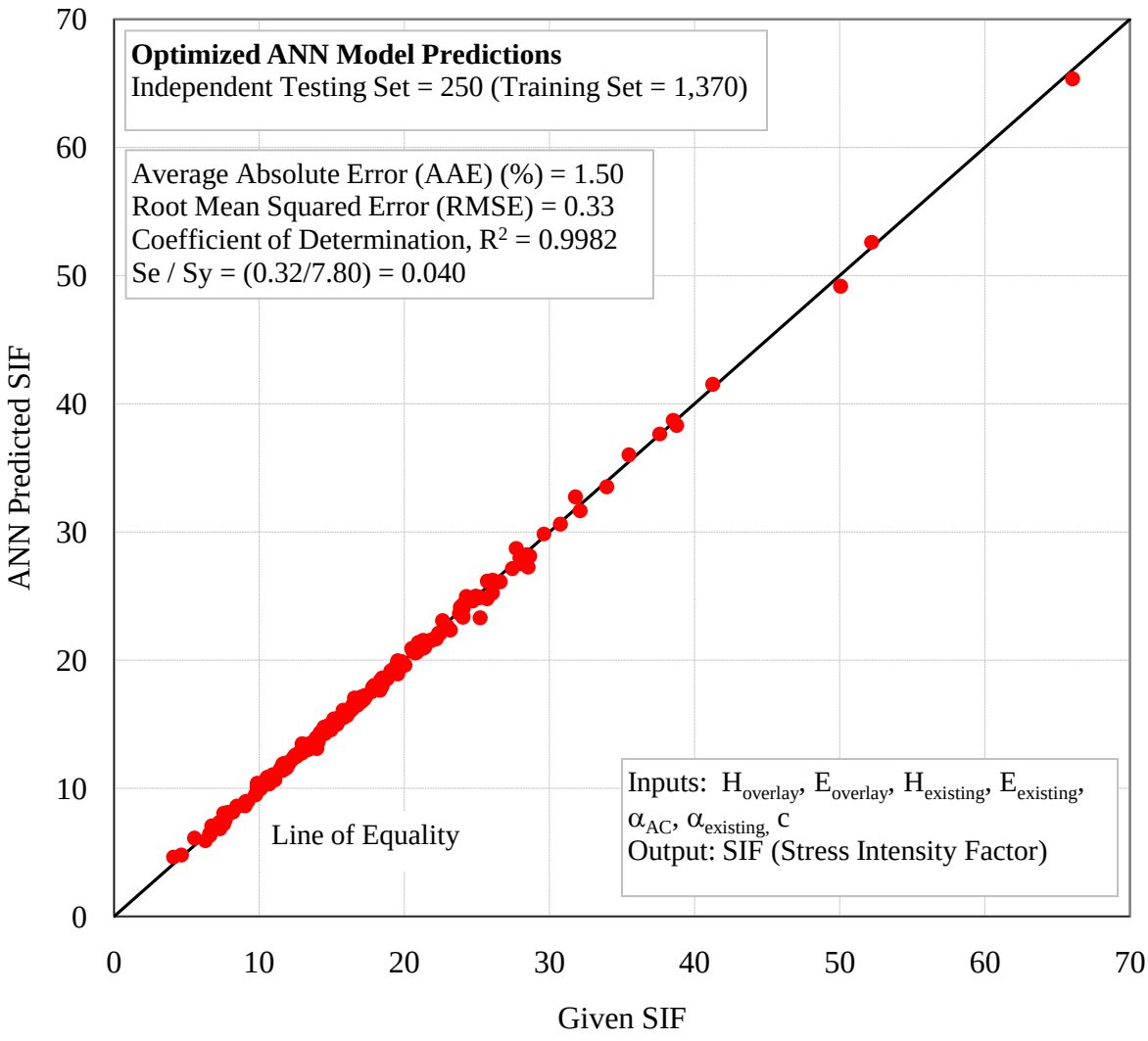

Figure F-4. ANN Model of thermal stress intensity factors for asphalt overlays over cracked asphalt surface layer.

2. HMA Overlay on Jointed Concrete Pavement

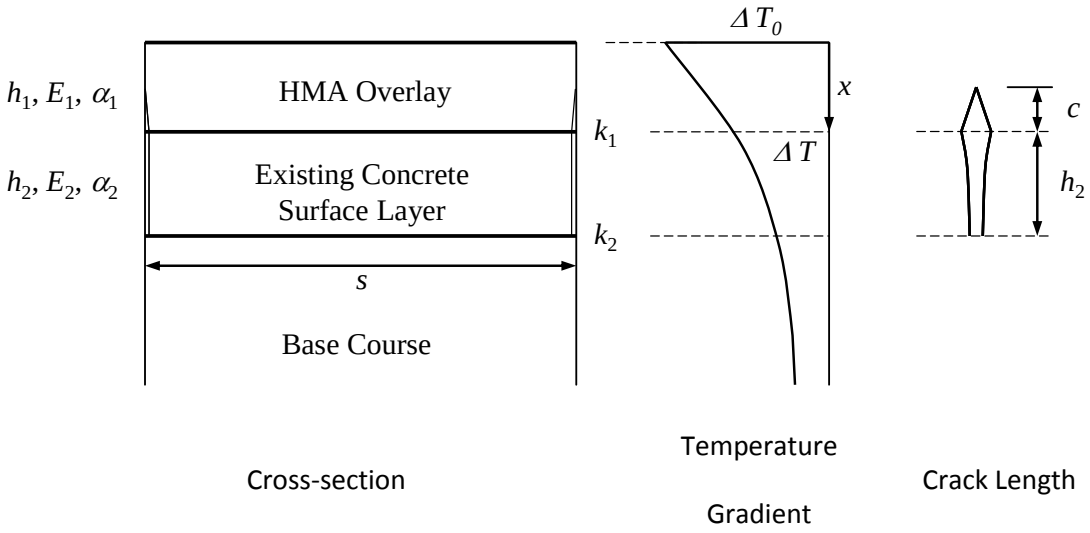

Figure F-5. Diagrams of HMA overlay on jointed concrete pavement-thermal.

Table F-2. Thermal stress variables in HMA overlay on jointed concrete pavement system.

Variable		Unit	Value
Overlay Layer	Thickness (h_1)	mm	38, 75, 150
	Modulus (E_1)	MPa	70, 300, 700
	Coefficient of Thermal Expansion (α_1)	strain/°C	2×10^{-5}, 4×10^{-5}
Interface Condition (k_1)		-	1.0
Existing Surface	Thickness (h_2)	mm	200, 300, 350
	Modulus (E_2)	MPa	20,000, 30,000, 40,000
	Coefficient of Thermal Expansion (α_2)	strain/°C	1×10^{-5}, 2×10^{-5}
Interface Condition (k_2)		-	0, 0.5, 1.0
Temperature Differential (ΔT_0)		°C	30
Half Slab Length between Joints (s/2)		mm	2250, 4500, 7500
Ratio of Crack Length to Layer Thickness (c / h_1)		-	0.1, 0.3, 0.5, 0.7, 0.9

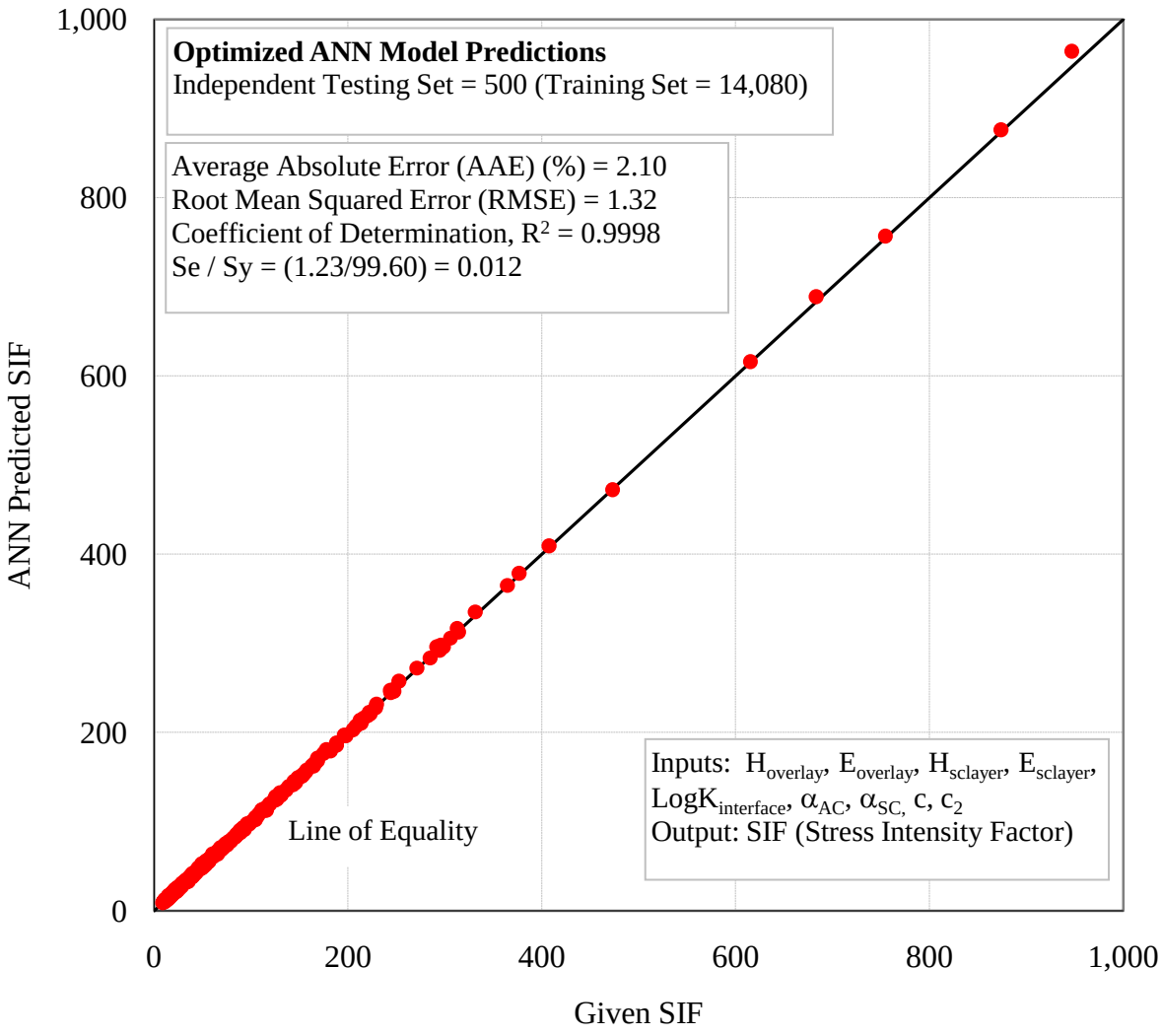

Figure F-6. ANN model of stress intensity factors of asphalt overlay on jointed concrete pavement.

3. HMA Overlay on Asphalt Concrete Pavement with Seal Coat or Friction Course-Thermal

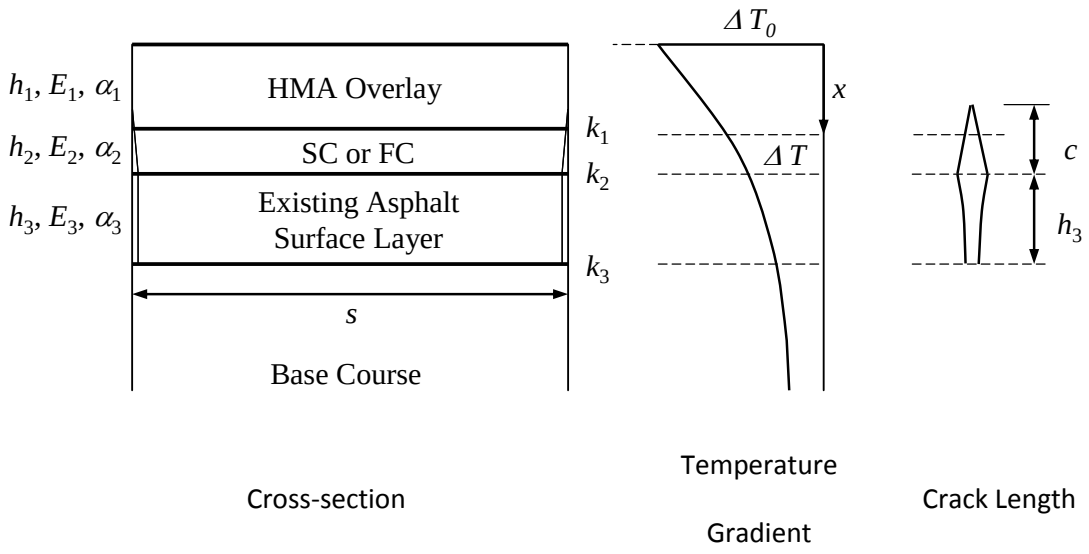

Figure F-7. Diagram of HMA overlay on asphalt concrete pavement with SC or FC-thermal.

Table F-3. Thermal stress-variables in HMA overlay on asphalt concrete pavement with SC or FC system.

Variable		Unit	Value
Overlay Layer	Thickness (h_1)	mm	38, 75, 150
	Modulus (E_1)	MPa	70, 300, 700
	Coefficient of Thermal Expansion (α_1)	strain/°C	2×10^{-5}, 4×10^{-5}
Interface Condition (k_1)		-	1.0
SC or FC	Thickness (h_2)	mm	15, 60
	Modulus (E_2)	MPa	50, 300
	Coefficient of Thermal Expansion (α_2)	strain/°C	2×10^{-5}, 4×10^{-5}
Interface Condition (k_2)		-	1.0
Existing Surface	Thickness (h_3)	mm	100, 200, 300
	Modulus (E_3)	MPa	70, 300, 700
	Coefficient of Thermal Expansion (α_3)	strain/°C	2×10^{-5}, 4×10^{-5}
Interface Condition (k_3)		-	1.0
Temperature Differential (ΔT_0)		°C	30
Half Crack Spacing (s/2)		mm	4500
Ratio of Crack Length to Layer Thickness (c /[h_1+h_2])		-	0.1 , 0.3, 0.5, 0.7, 0.9

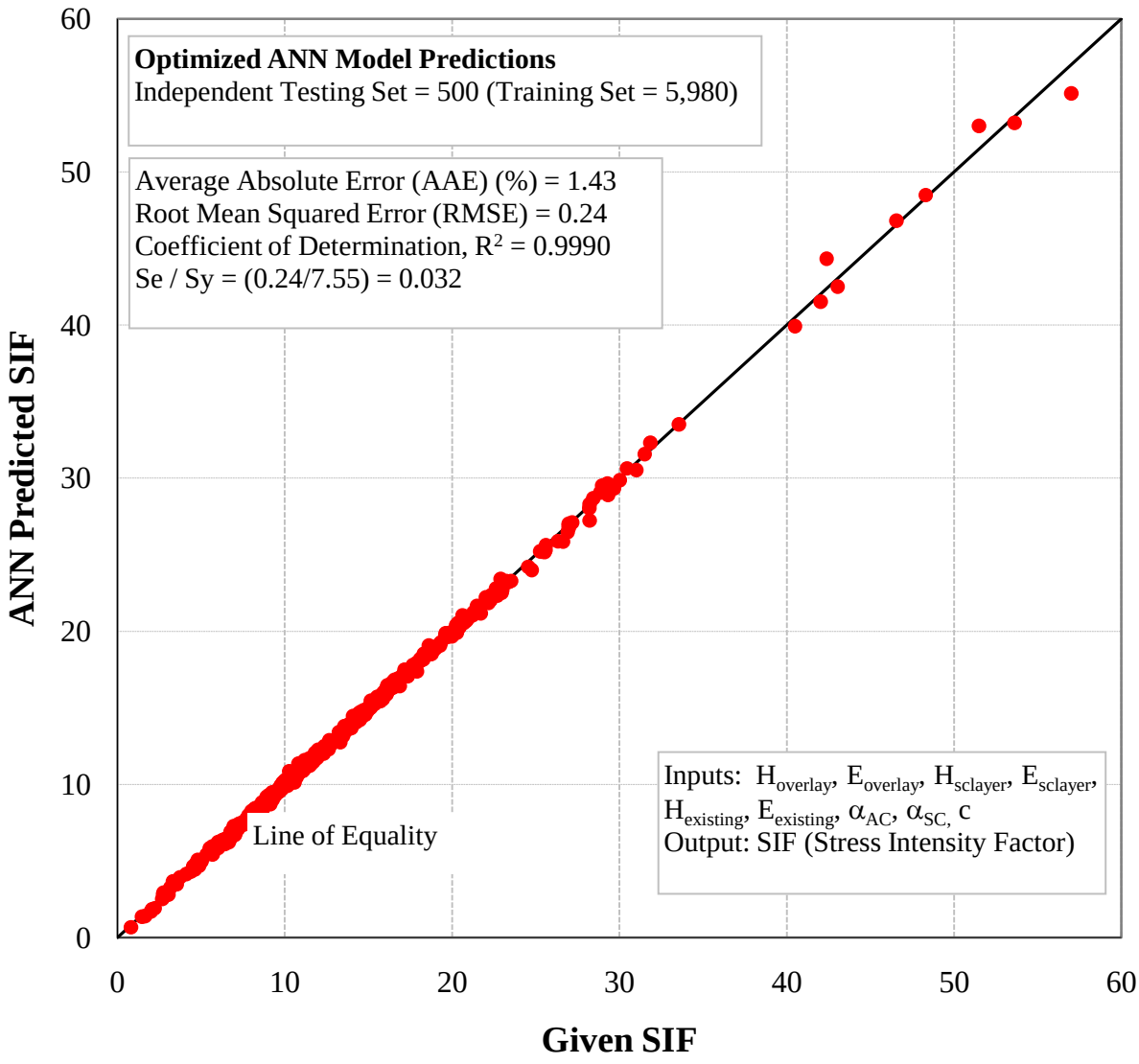

Figure F-8. ANN model of stress intensity factor for asphalt overlay over seal coat or open graded friction course over cracked asphalt surface layer.

4. HMA Overlay on Asphalt Concrete Pavement with Reinforcing Interlayer on Level-up and Beneath Overlay

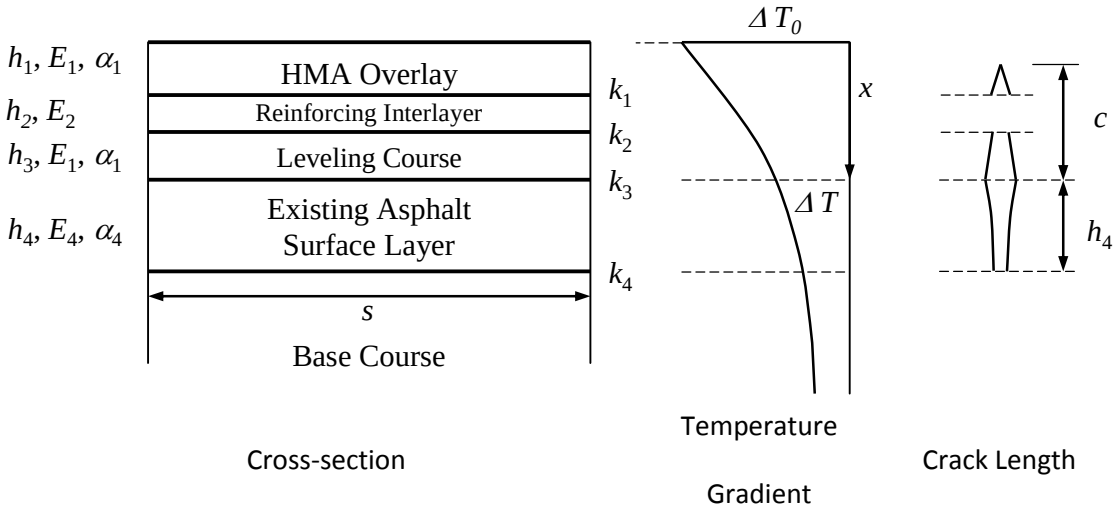

Figure F-9. Diagram of HMA overlay on asphalt concrete pavement with reinforcing interlayer beneath overlay-thermal.

As noted in Table F-4, three levels of interlayer reinforcing were modeled using three different ANN models. In the following three figures, the fit that was achieved with each of the three levels of reinforcing are illustrated.

Table F-4. Thermal stress variables in HMA overlay on asphalt concrete pavement with reinforcing interlayer on level-up and beneath overlay system.

Variable		Unit	Value
Overlay Layer	Thickness (h_1)	mm	38, 75, 150
	Modulus (E_1)	MPa	70, 300, 700
	Coefficient of Thermal Expansion (α_1)	strain/°C	2×10^{-5}, 4×10^{-5}
Interface Condition (k_1)		-	1.0
Reinf. Interlayer	[Thickness (h_2), Modulus (E_2)]	[mm, MPa]	[2.5, 10000], [1, 1250], [2, 150]
Interface Condition (k_2)		-	0
Leveling Course	Thickness (h_3)	mm	25, 50
Interface Condition (k_3)		-	1.0
Existing Surface	Thickness (h_4)	mm	100, 200, 300
	Modulus (E_4)	MPa	70, 300, 700
	Coefficient of Thermal Expansion (α_4)	strain/°C	2×10^{-5}, 4×10^{-5}
Interface Condition (k_4)		-	1.0
Temperature Differential (ΔT_0)		°C	30
Half Crack Spacing (s/2)		mm	4500
Ratio of Crack Length to Layer Thickness (c / [h_1+h_3])		-	0.1 , 0.3, 0.5, 0.7, 0.9

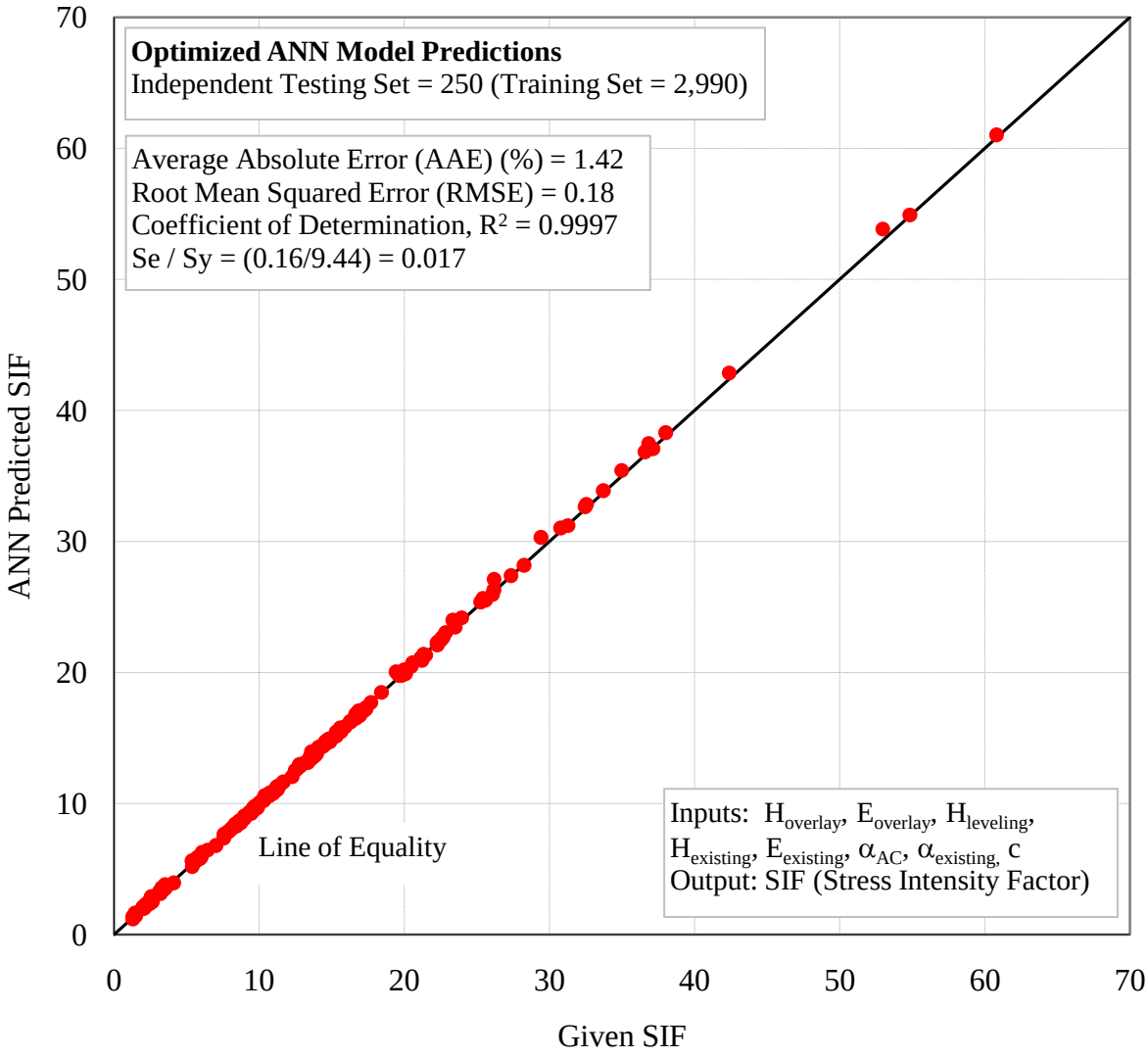

Figure F-10. ANN models for stress intensity factors for overlays over cracked asphalt surface layer–low interlayer reinforcing stiffness level-thermal.

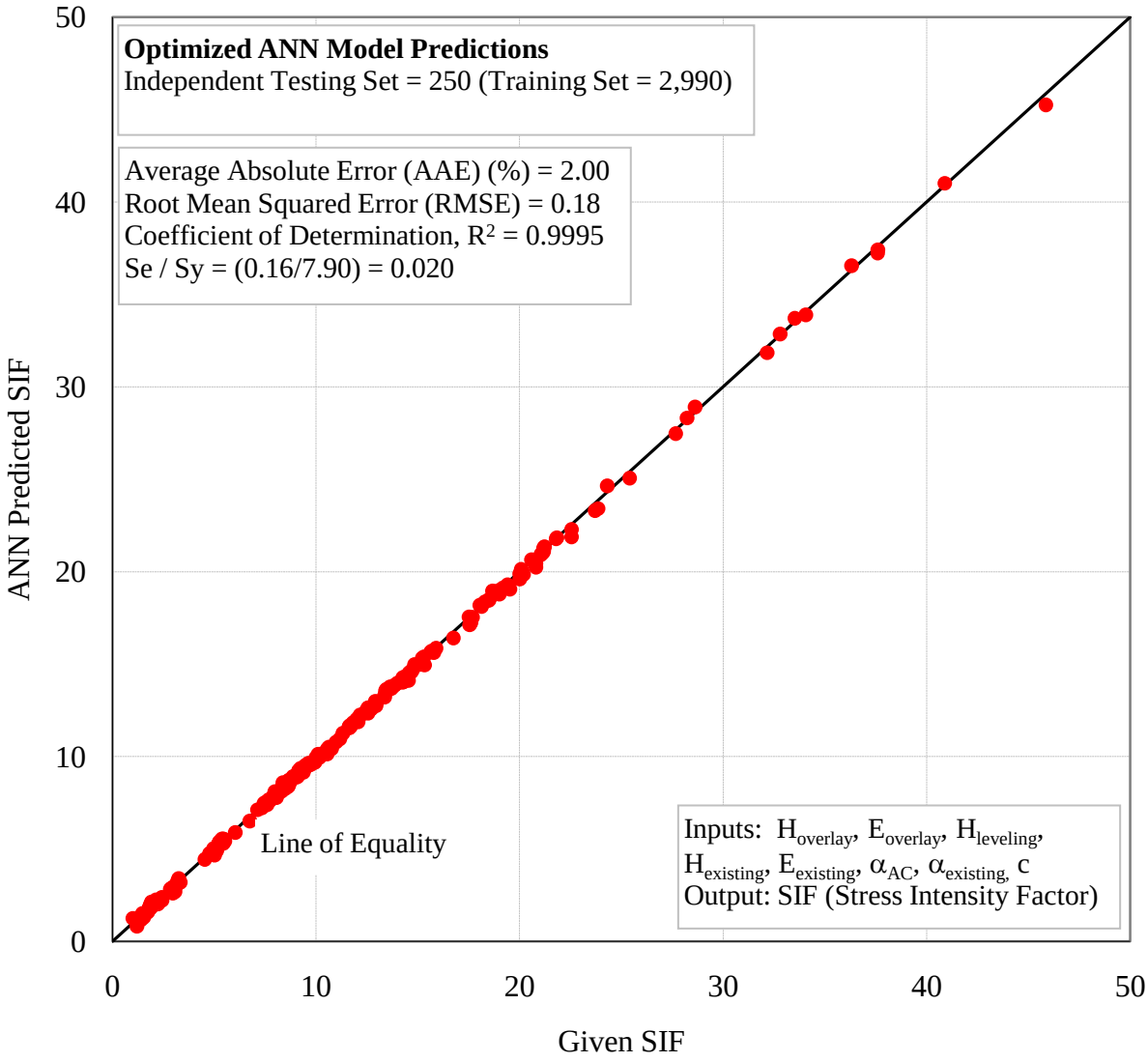

Figure F-11. ANN models for stress intensity factors for asphalt overlays over cracked asphalt surface layer–medium interlayer reinforcing stiffness level-thermal.

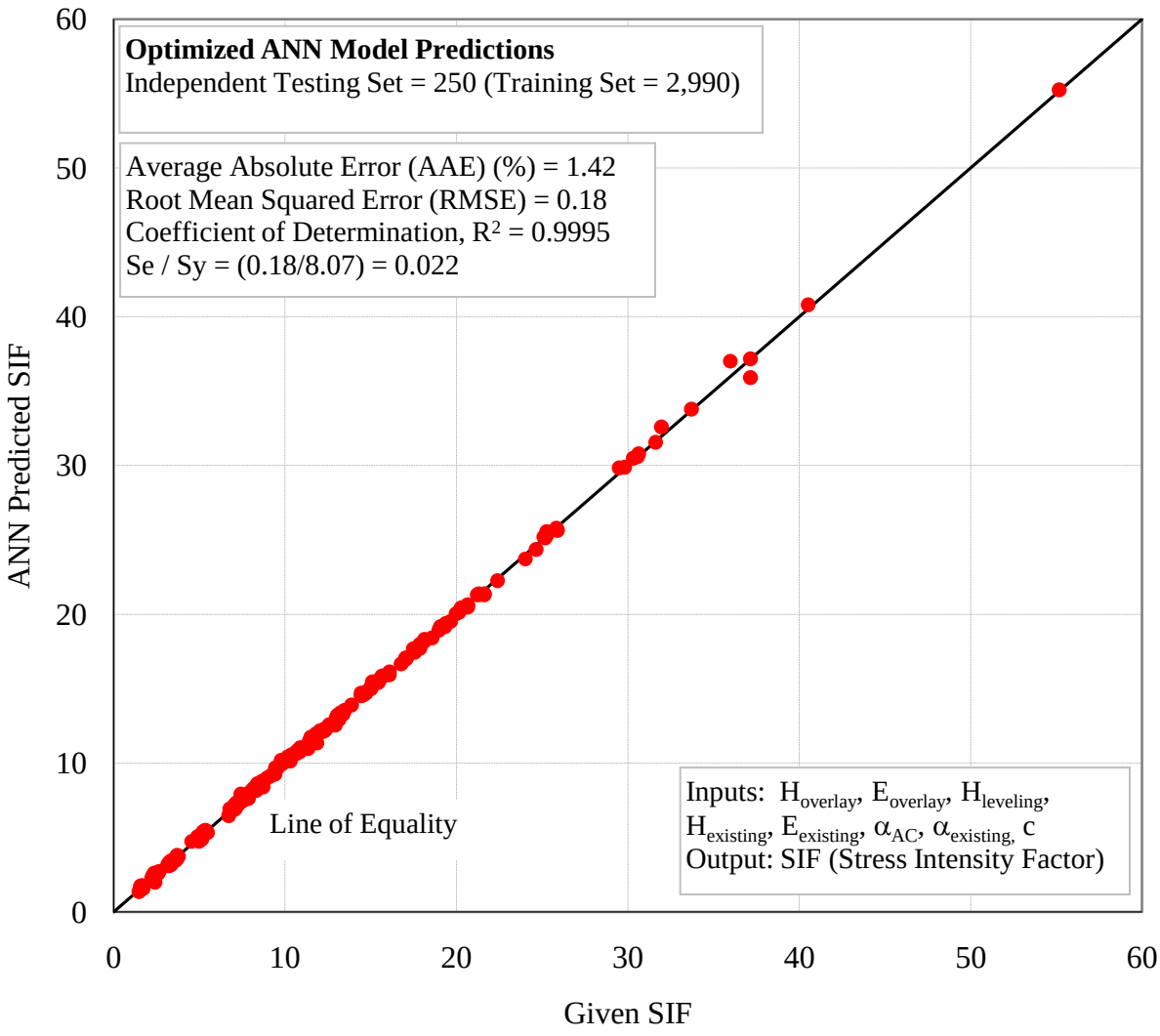

Figure F-12. ANN Models for stress intensity factors for asphalt overlays over cracked asphalt surface layer–high interlayer reinforcing stiffness level-thermal.

The four shearing reflection cracking cases are shown in Figures F-13 through F-22 and the companion tables of variables, Tables F-5 through F-8. When the shearing stress intensity factor reaches a peak as the tire both approaches and leaves the vicinity of the reflection crack, there is always a bending stress intensity factor also present at the tip of the crack. This explains why there is a "Shearing Part" and a "Bending Part" of the shearing stress intensity factor models and graphs. Having analyzed the bending stress intensity factors as the tire approaches, travels

over, and leaves the vicinity of the reflection crack has allowed the use of the stress intensity factor wave form which is called for in Schapery's theory of crack growth in viscoelastic media.

SHEARING REFLECTION CRACKING CASES

5. HMA Overlay on Asphalt Concrete Pavement (Single Axle – Single Tire)

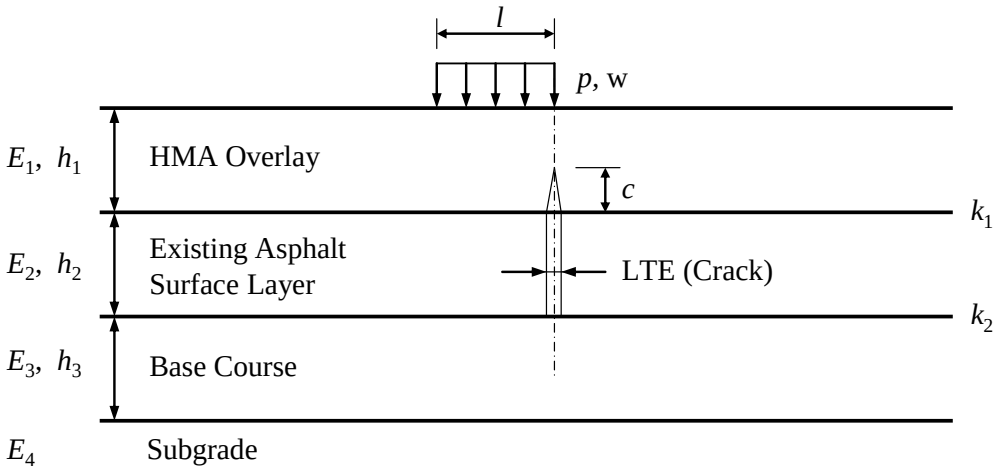

Figure F-13. Diagram of HMA overlay on asphalt concrete pavement-shearing.

Table F-5. Shearing stress variables in HMA overlay on asphalt concrete pavement system.

Variable		Unit	Value
Overlay Layer	Thickness (h_1)	mm	38, 75, 150
	Modulus (E_1)	MPa	1,000, 10,000
Interface Condition (k_1)		-	1.0
Existing Surface	Thickness (h_2)	mm	100, 200, 300
	Modulus (E_2)	MPa	500, 5,000
Interface Condition (k_2)		-	1.0
Base Course	Thickness (h_3)	mm	100, 1,000
	Modulus (E_3)	MPa	150, 600
Subgrade	Modulus (E_4)	MPa	30, 150
Traffic Load	Length of Tire Patch (l)	mm	64, 305, 406
	Tire Pressure (p)	psi	96
	Tire Width (w)	mm	200
Load Transfer Efficiency (LTE)		-	0.3, 0.7, 1.0
Ratio of Crack Length to Layer Thickness (c / h_1)		-	0.1, 0.3, 0.5, 0.7, 0.9

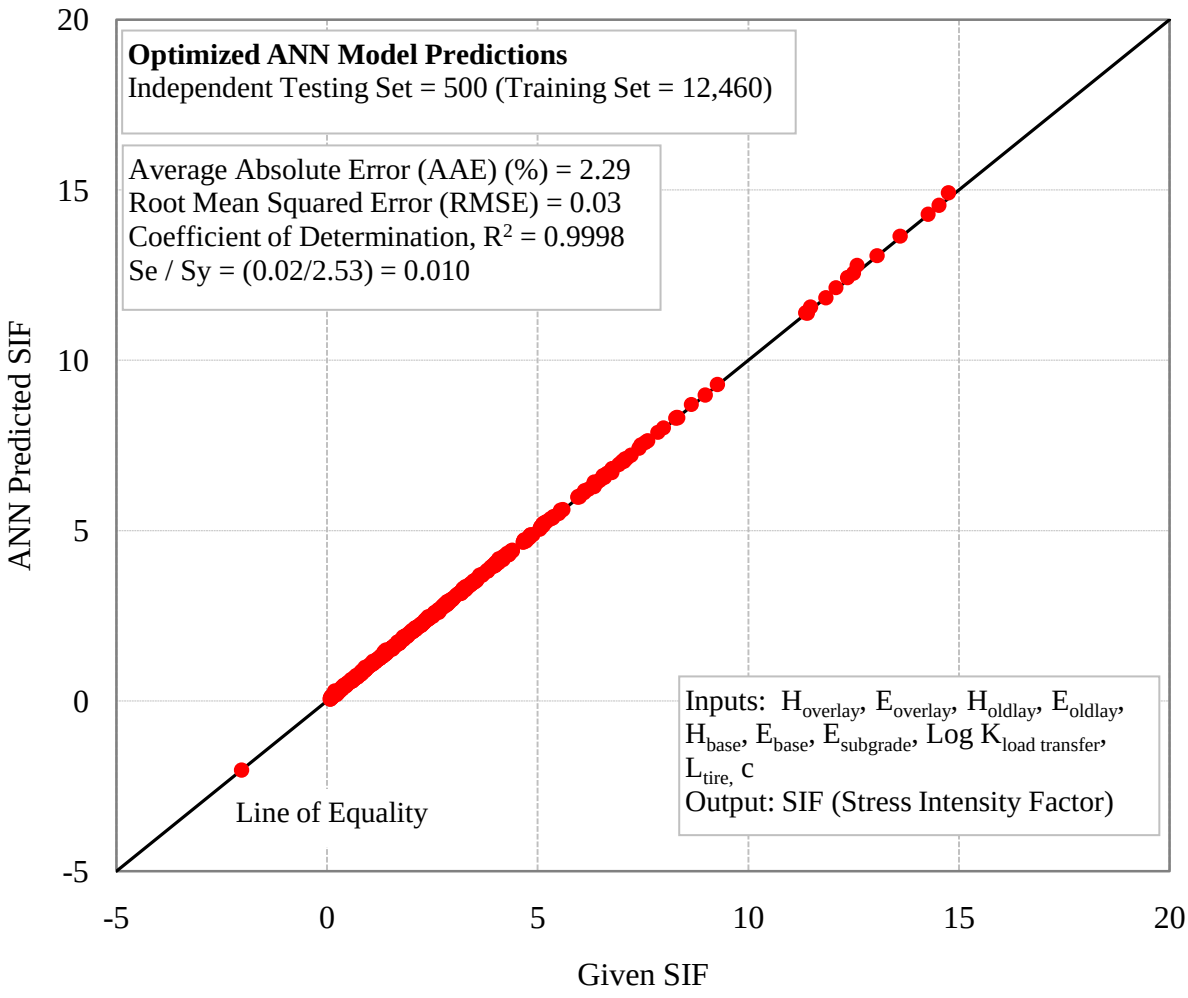

Figure F-14. ANN model of the shearing part of the shearing stress intensity factors for asphalt overlays over cracked asphalt surface layer (single axle-single tire).

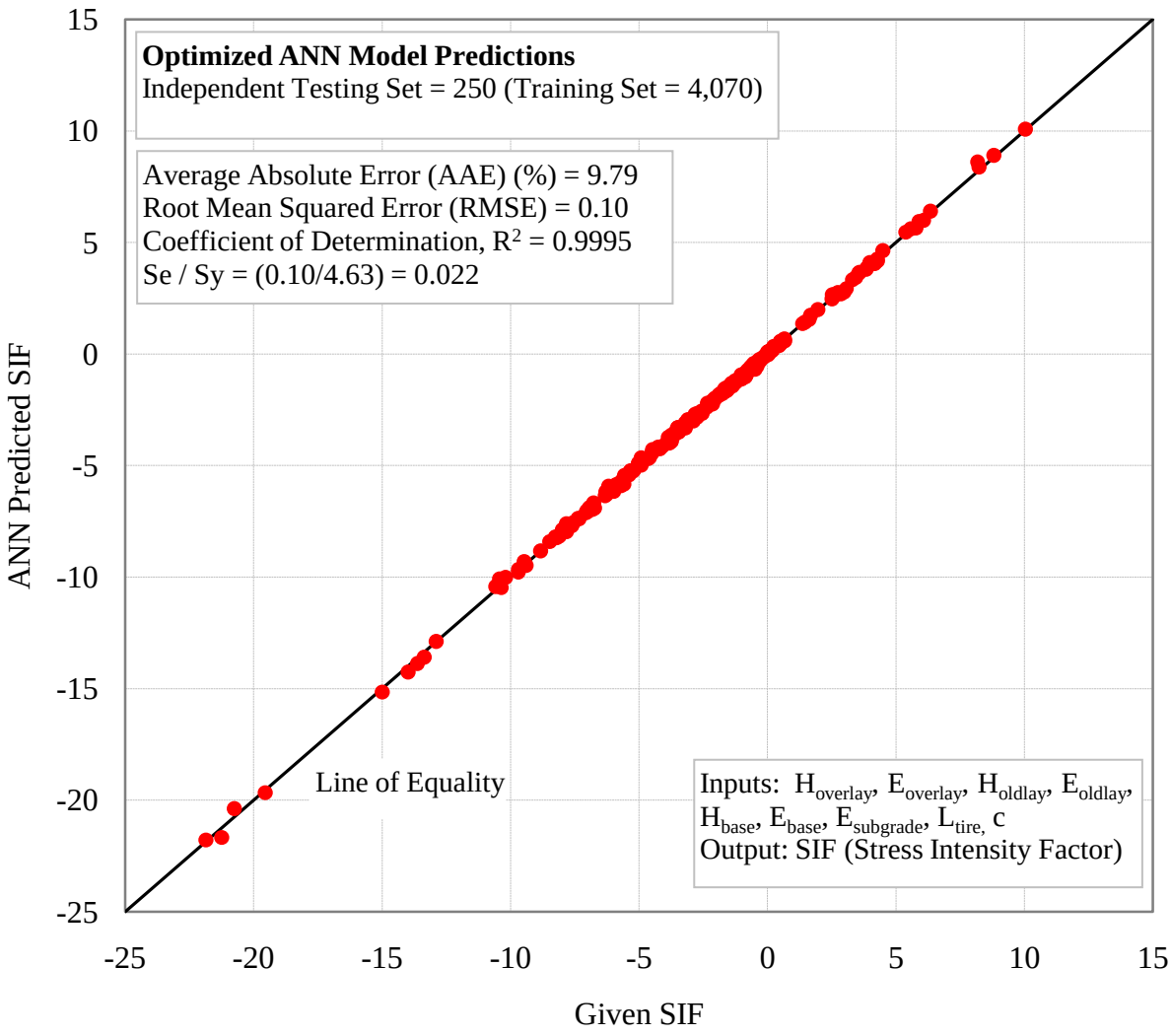

Figure F-15. ANN model of the bending part of the shearing stress intensity factors for asphalt overlays over cracked asphalt surface layer (single axle–single tire).

6. HMA Overlay on Asphalt Concrete Pavement (Single Axle – Dual Tires)

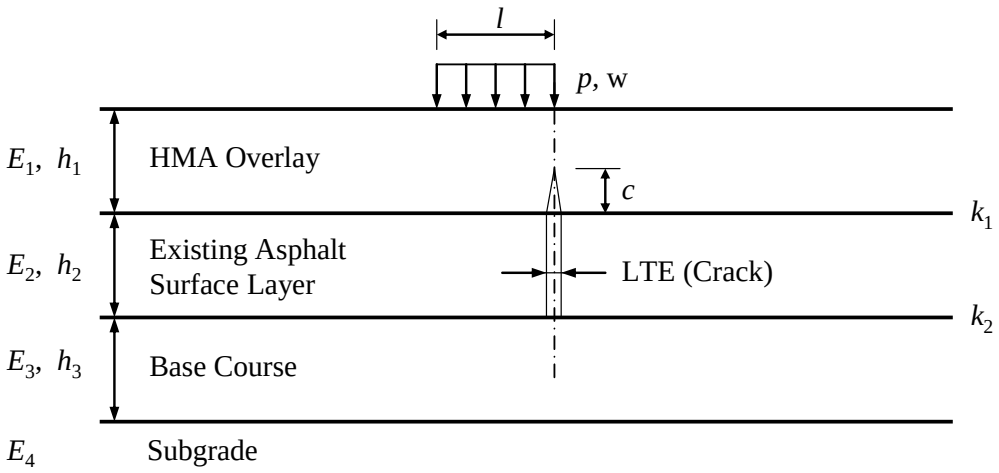

Figure F-16. Diagram of HMA overlay on asphalt concrete pavement-shearing.

Table F-6. Shearing stress variables in HMA overlay on asphalt concrete pavement system.

Variable		Unit	Value
Overlay Layer	Thickness (h_1)	mm	38, 75, 150
	Modulus (E_1)	MPa	1,000, 10,000
Interface Condition (k_1)		-	1.0
Existing Surface	Thickness (h_2)	mm	100, 200, 300
	Modulus (E_2)	MPa	500, 5,000
Interface Condition (k_2)		-	1.0
Base Course	Thickness (h_3)	mm	100, 1,000
	Modulus (E_3)	MPa	150, 600
Subgrade	Modulus (E_4)	MPa	30, 150
Traffic Load	Length of Tire Patch (l)	mm	64, 127, 229
	Tire Pressure (p)	psi	96
	Tire Width (w)	mm	222
Load Transfer Efficiency (LTE)		-	0.3, 0.7, 1.0
Ratio of Crack Length to Layer Thickness (c / h_1)		-	0.1, 0.3, 0.5, 0.7, 0.9

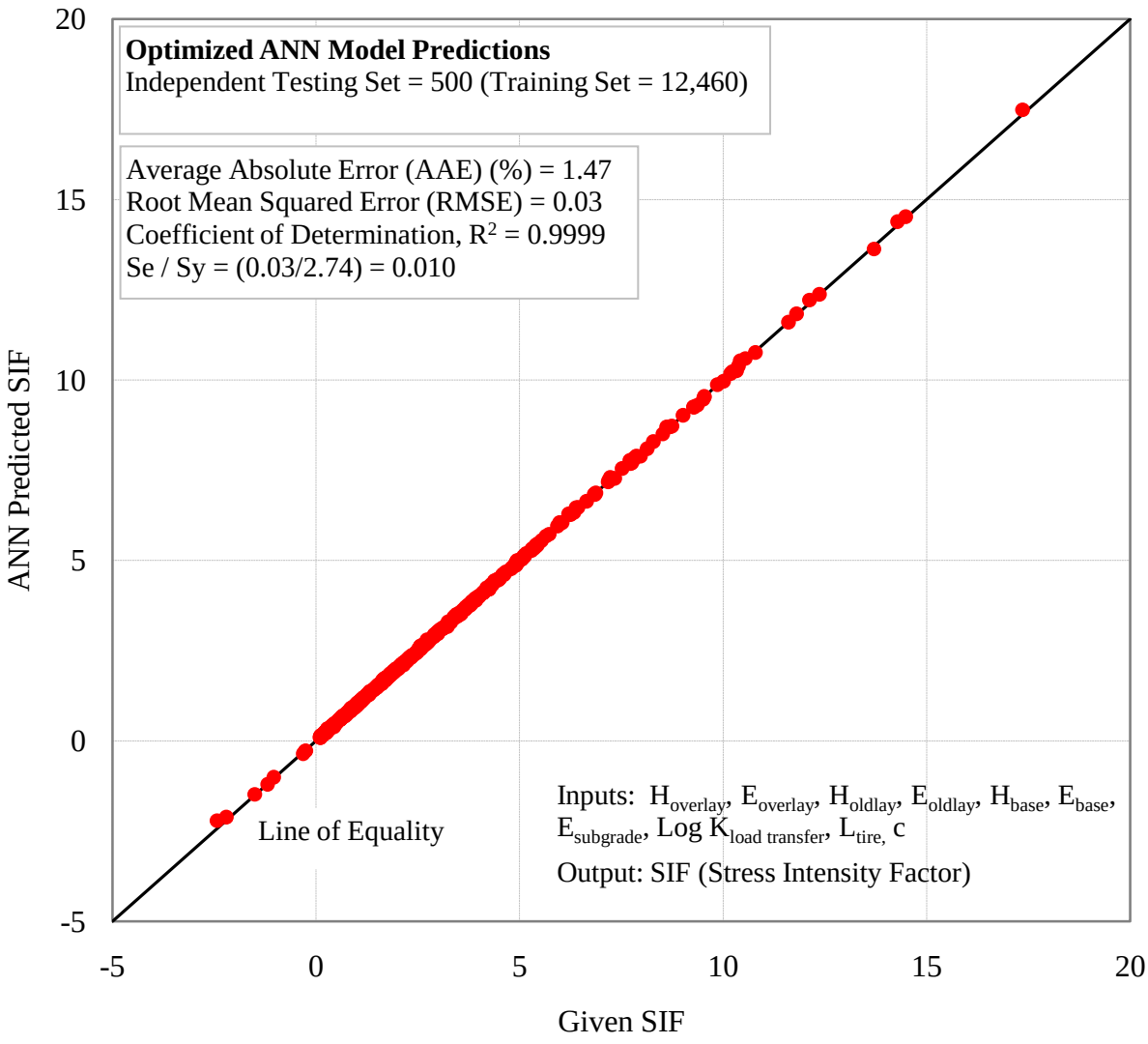

Figure F-17. ANN model of the shearing part of the shearing stress intensity factors for asphalt overlays over cracked asphalt surface layer (single axle–dual tire).

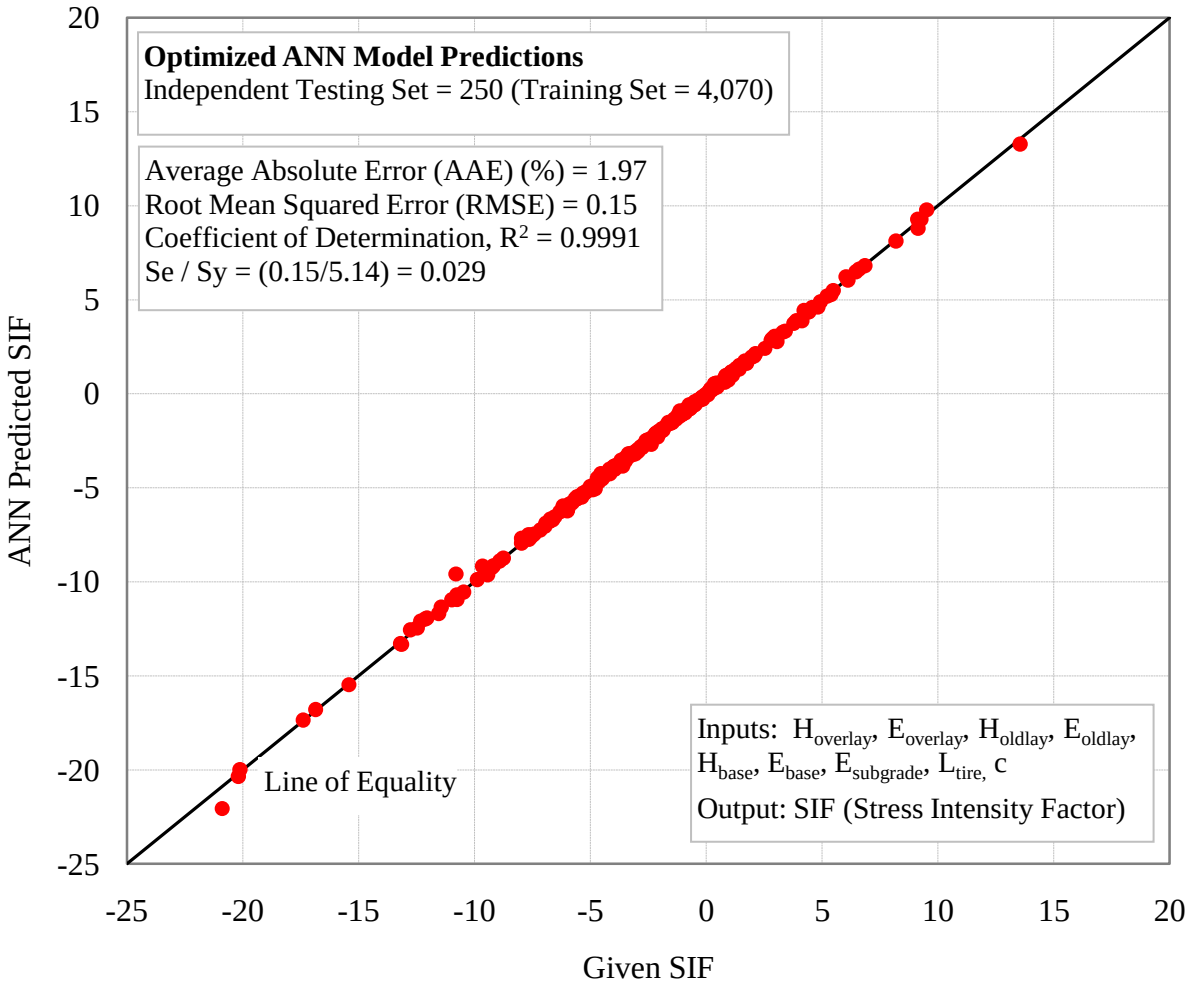

Figure F-18. ANN model of the bending part of the shearing stress intensity factors for asphalt overlays over crack asphalt surface layer (single axle–dual tire).

7. HMA Overlay on Jointed Concrete Pavement (Single Axle – Single Tire)

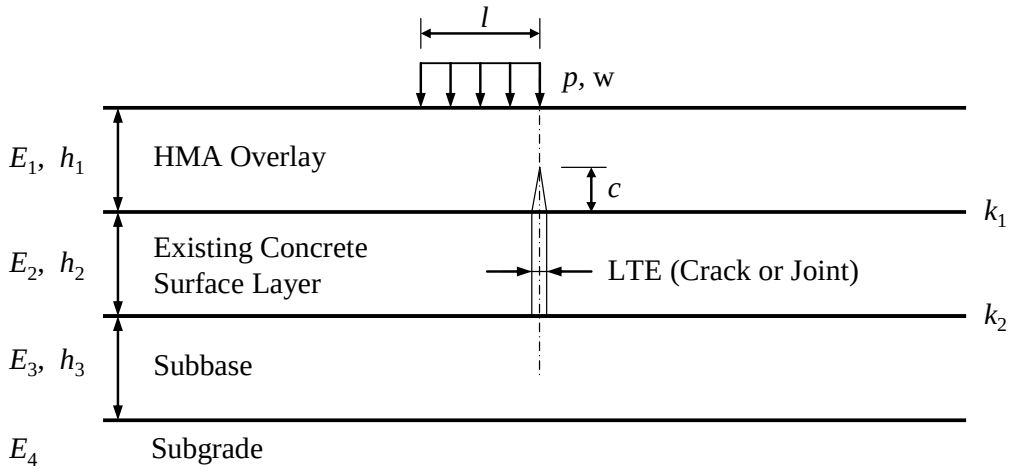

Figure F-19. Diagram of HMA overlay on jointed concrete pavement-shearing.

Table F-7. Shearing stress variables in HMA overlay on jointed concrete pavement system.

Variable		Unit	Value
Overlay Layer	Thickness (h_1)	mm	38, 75, 150
	Modulus (E_1)	MPa	1,000, 10,000
Interface Condition (k_1)		-	1.0
Existing Surface	Thickness (h_2)	mm	200, 300, 350
	Modulus (E_2)	MPa	20,000, 30,000, 40,000
Interface Condition (k_2)		-	0.5
Subbase	Thickness (h_3)	mm	100, 1,000
	Modulus (E_3)	MPa	150, 600
Subgrade	Modulus (E_4)	MPa	30, 150
Traffic Load	Length of Tire Patch (l)	mm	64, 305, 406
	Tire Pressure (p)	psi	96
	Tire Width (w)	mm	200
Load Transfer Efficiency (LTE)		-	0.3, 0.7, 1.0
Ratio of Crack Length to Layer Thickness (c / h_1)		-	0.1, 0.3, 0.5, 0.7, 0.9

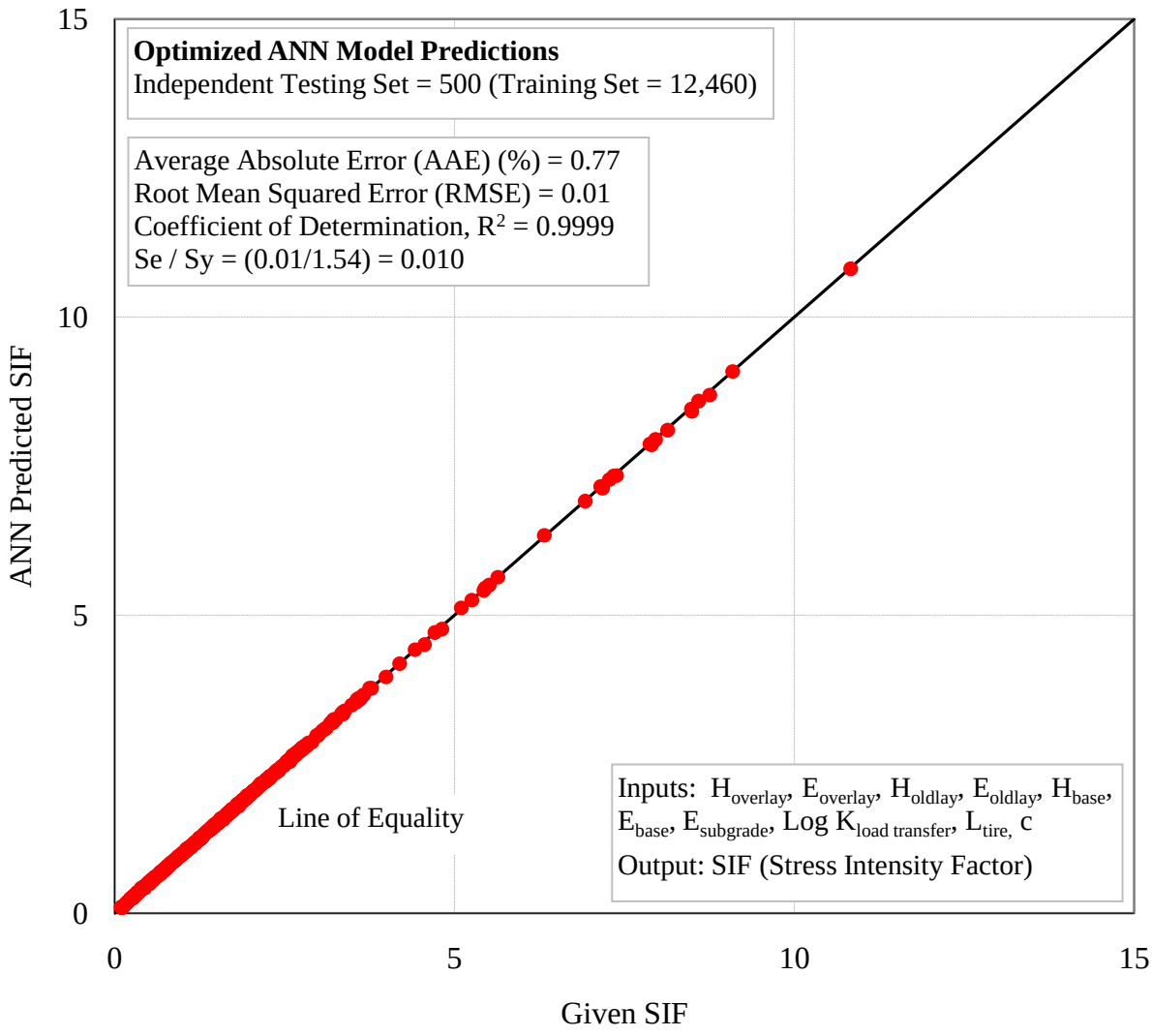

Figure F-20. ANN model of the shearing stress intensity factors for asphalt overlays over jointed concrete surface layer (single axle–single tire).

8. HMA Overlay on Jointed Concrete Pavement (Single Axle – Dual Tires)

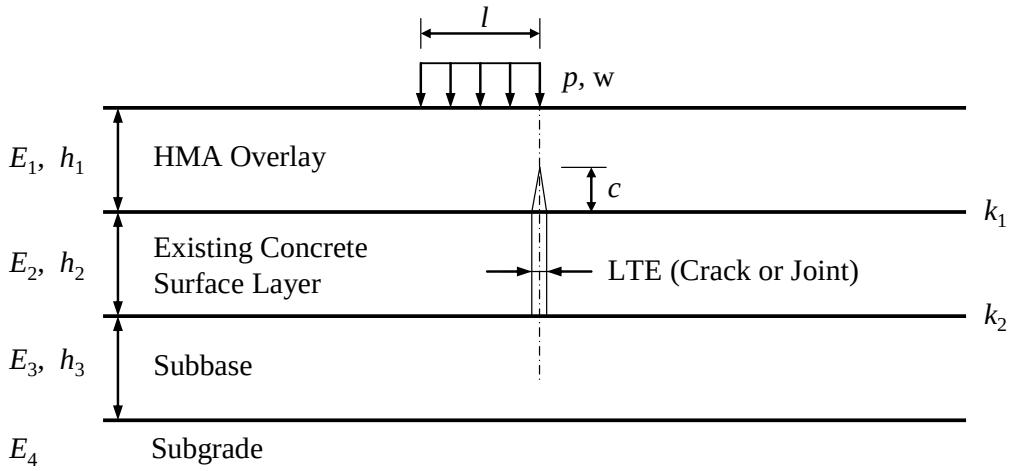

Figure F-21. Diagram of HMA overlay on jointed concrete pavement-shearing.

Table F-8. Shearing stress variables in HMA overlay on jointed concrete pavement system.

Variable		Unit	Value
Overlay Layer	Thickness (h_1)	mm	38, 75, 150
	Modulus (E_1)	MPa	1,000, 10,000
Interface Condition (k_1)		-	1.0
Existing Surface	Thickness (h_2)	mm	200, 300, 350
	Modulus (E_2)	MPa	20,000, 30,000, 40,000
Interface Condition (k_2)		-	0.5
Subbase	Thickness (h_3)	mm	100, 1,000
	Modulus (E_3)	MPa	150, 600
Subgrade	Modulus (E_4)	MPa	30, 150
Traffic Load	Length of Tire Patch (l)	mm	64, 127, 229
	Tire Pressure (p)	psi	96
	Tire Width (w)	mm	222
Load Transfer Efficiency (LTE)		-	0.3, 0.7, 1.0
Ratio of Crack Length to Layer Thickness (c / h_1)		-	0.1, 0.3, 0.5, 0.7, 0.9

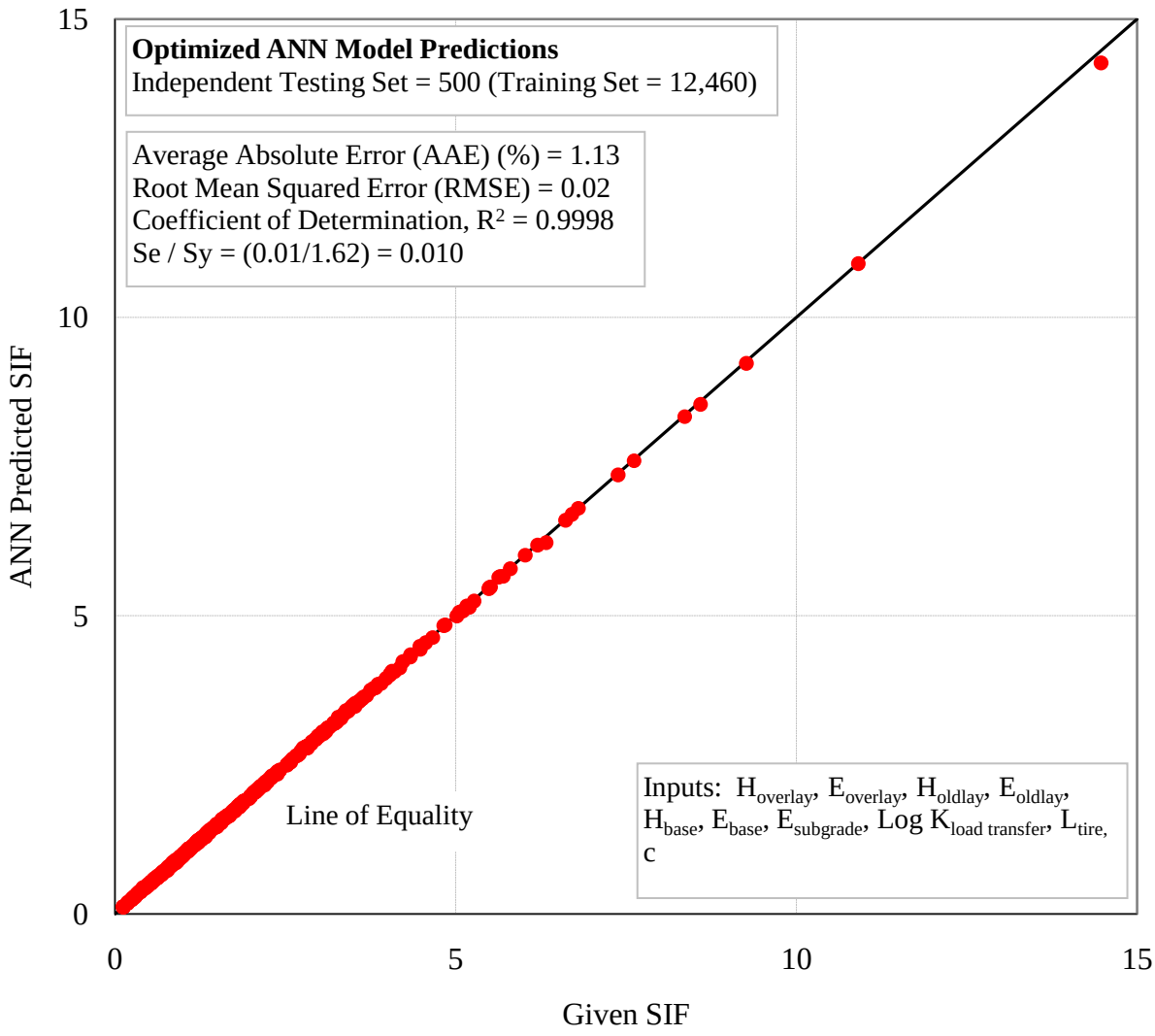

Figure F-22. ANN model of the shearing stress intensity factors for asphalt overlays over jointed concrete surface layer (single axle – dual tire).

The four bending reflection cracking stress intensity factor cases are shown in Figures F-23 through F-32 and the companion tables of variables shown in Tables F-9 through F-12.

BENDING REFLECTION CRACKING CASES

9. HMA Overlay on Asphalt Concrete Pavement (Single Axle – Single Tire)

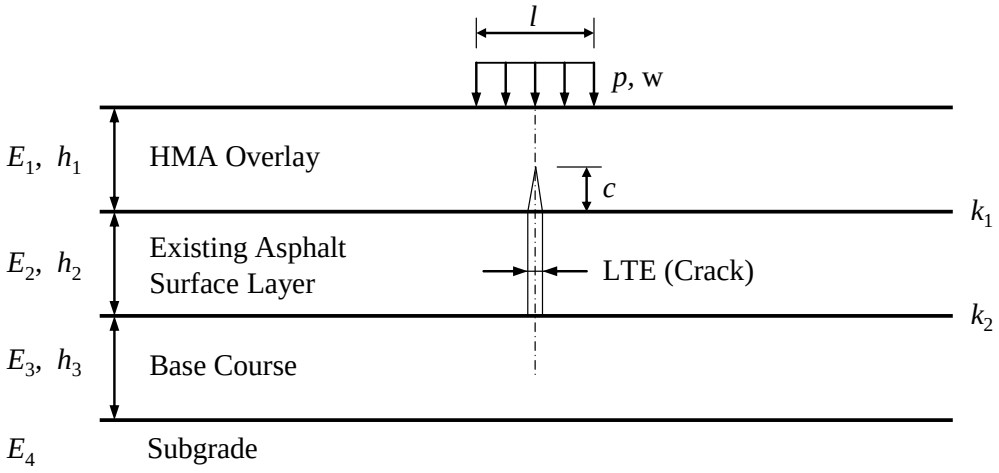

Figure F-23. Diagram of HMA overlay on asphalt concrete pavement-bending.

Table F-9. Bending stress variables in HMA overlay on asphalt concrete pavement system.

Variable		Unit	Value
Overlay Layer	Thickness (h_1)	mm	38, 75, 150
	Modulus (E_1)	MPa	1000, 10,000
Interface Condition (k_1)		-	1.0
Existing Surface	Thickness (h_2)	mm	100, 200, 300
	Modulus (E_2)	MPa	500, 5,000
Interface Condition (k_2)		-	0.5
Base Course	Thickness (h_3)	mm	150, 600
	Modulus (E_3)	MPa	100, 1,000
Subgrade	Modulus (E_4)	MPa	30, 150
Traffic Load	Length of Tire Patch (l)	mm	64, 305, 406
	Tire Pressure (p)	psi	96
	Tire Width (w)	mm	200
Load Transfer Efficiency (LTE)		-	0.3, 0.7, 1.0
Ratio of Crack Length to Layer Thickness (c / h_1)		-	0.1, 0.3, 0.5, 0.7, 0.9

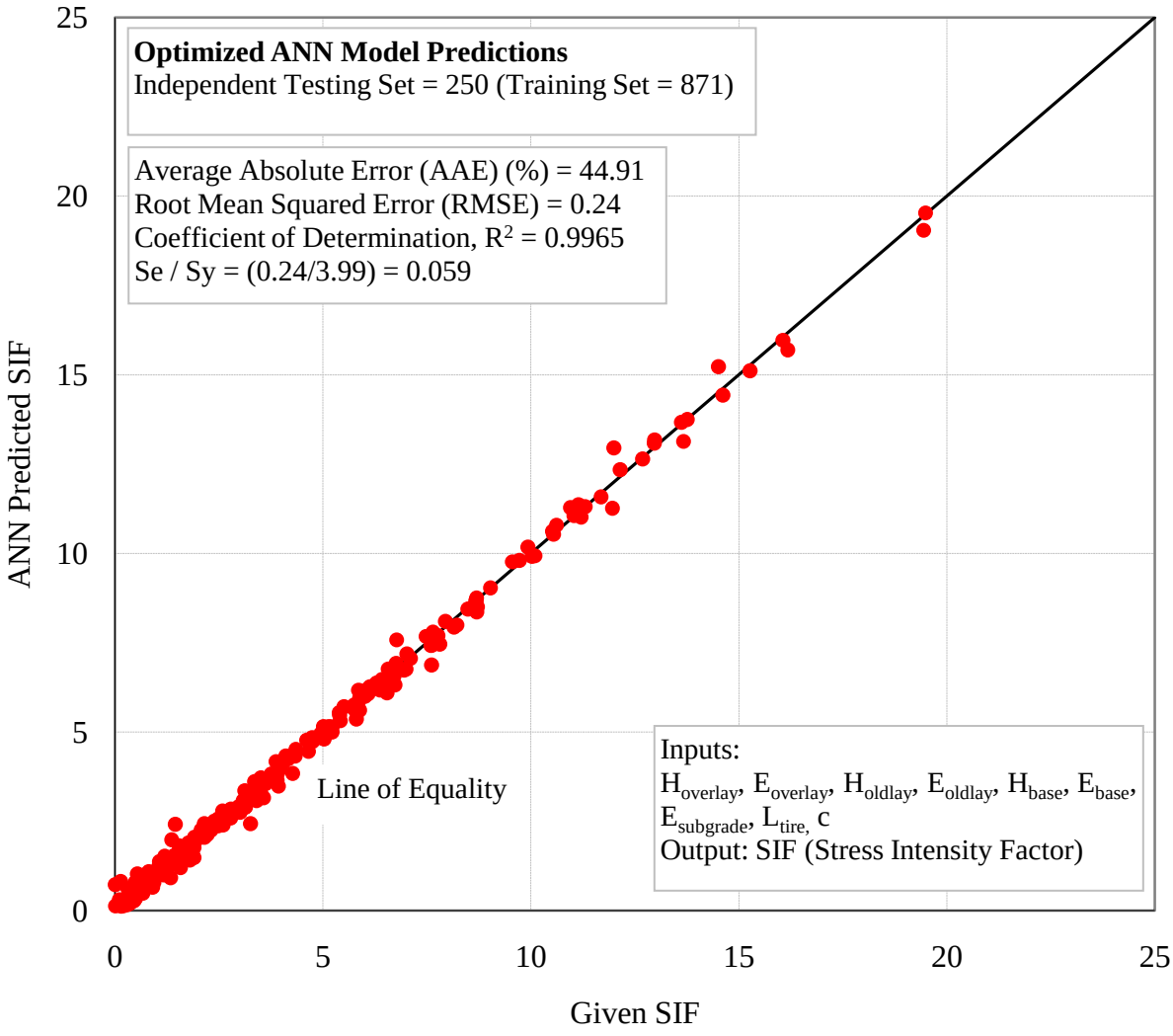

Figure F-24. ANN model of the positive part of the bending stress intensity factors for asphalt overlays over cracked asphalt surface layer (single axle–single tire).

As a matter of possible interest, the graph in Figure F-25 shows the results of an ANN model of both the positive and negative stress intensity factors for the single axle, single tire loading case.

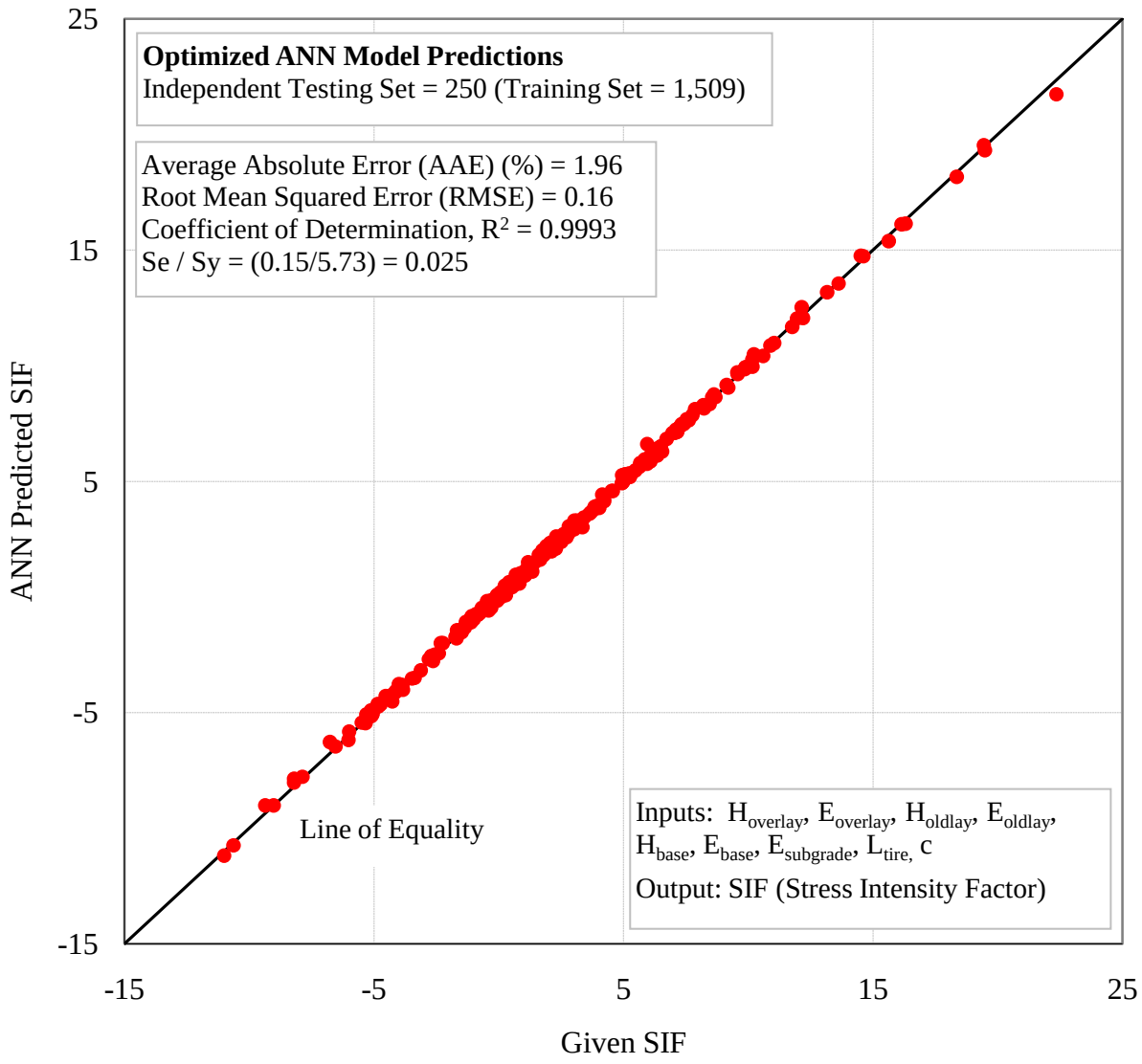

Figure F-25. ANN model of the positive and negative parts of the bending stress intensity factors for asphalt overlays over cracked asphalt surface layer (single axle–single tire).

10. HMA Overlay on Asphalt Concrete Pavement (Single Axle – Dual Tires)

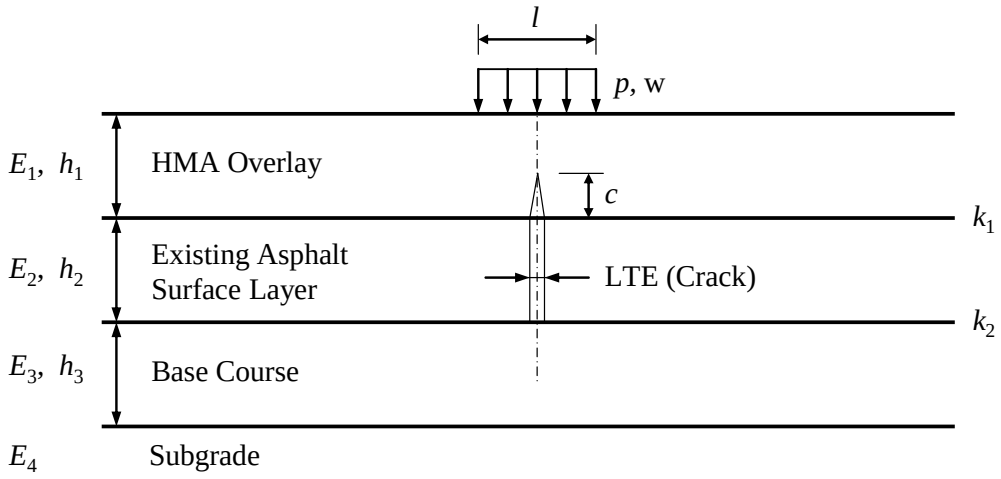

Figure F-26. Diagram of HMA overlay on asphalt concrete pavement-bending.

Table F-10. Bending stress variables in HMA overlay on asphalt concrete pavement system.

Variable		Unit	Value
Overlay Layer	Thickness (h_1)	mm	38, 75, 150
	Modulus (E_1)	MPa	1,000, 10,000
Interface Condition (k_1)		-	1.0
Existing Surface	Thickness (h_2)	mm	100, 200, 300
	Modulus (E_2)	MPa	500, 5000
Interface Condition (k_2)		-	0.5
Base Course	Thickness (h_3)	mm	150, 600
	Modulus (E_3)	MPa	100, 1,000
Subgrade	Modulus (E_4)	MPa	30, 150
Traffic Load	Length of Tire Patch (l)	mm	64, 127, 229
	Tire Pressure (p)	psi	96
	Tire Width (w)	mm	222
Load Transfer Efficiency (LTE)		-	0.3, 0.7, 1.0
Ratio of Crack Length to Layer Thickness (c / h_1)		-	0.1, 0.3, 0.5, 0.7, 0.9

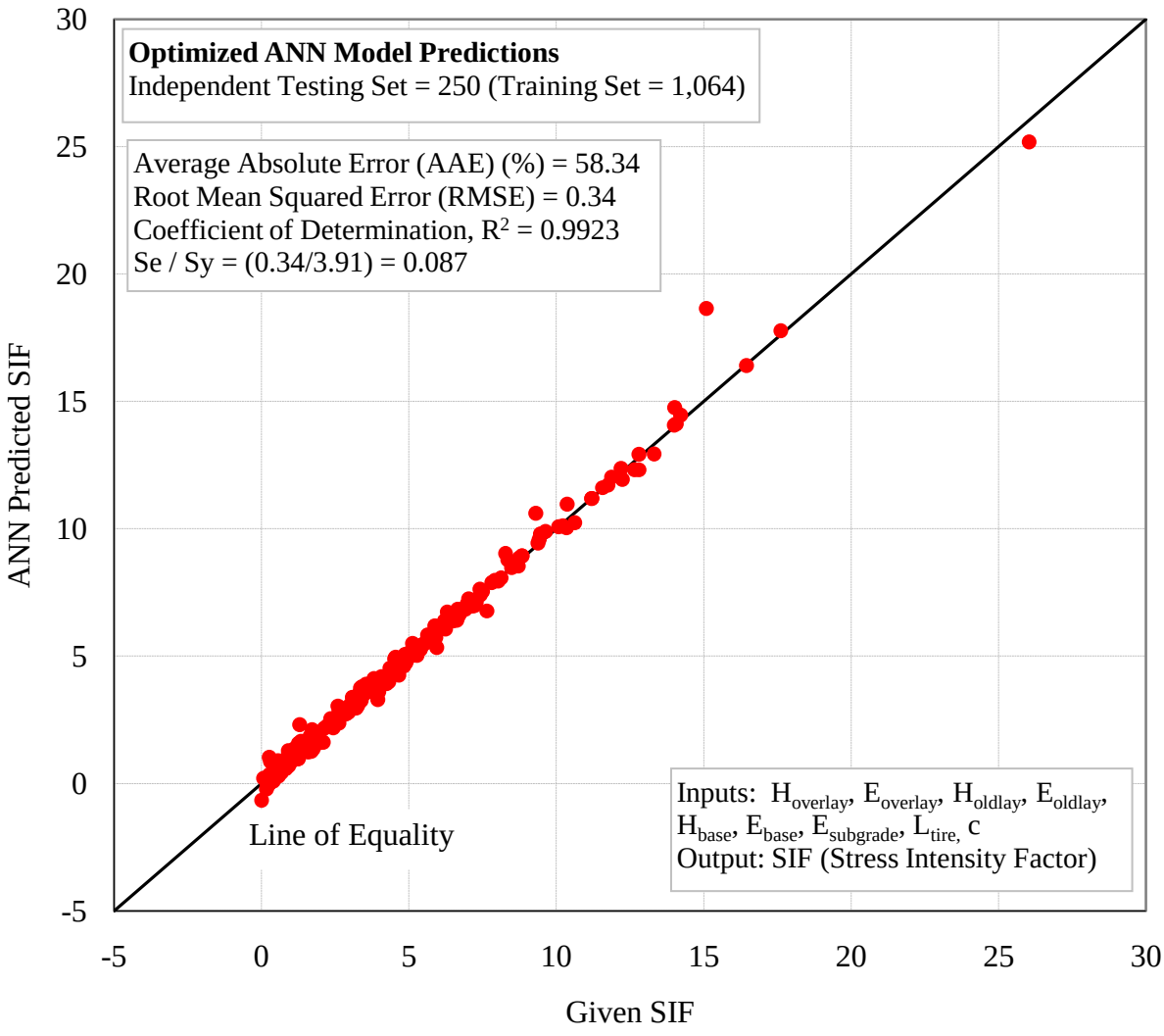

Figure F-27. ANN model of the positive part of the bending stress intensity factors for asphalt overlays over cracked asphalt surface layer (single axle–dual tire).

As with the single axle, single tire case, Figure F-28 presents the ANN model for both the positive and negative stress intensity factors for the single axle, dual tire case.

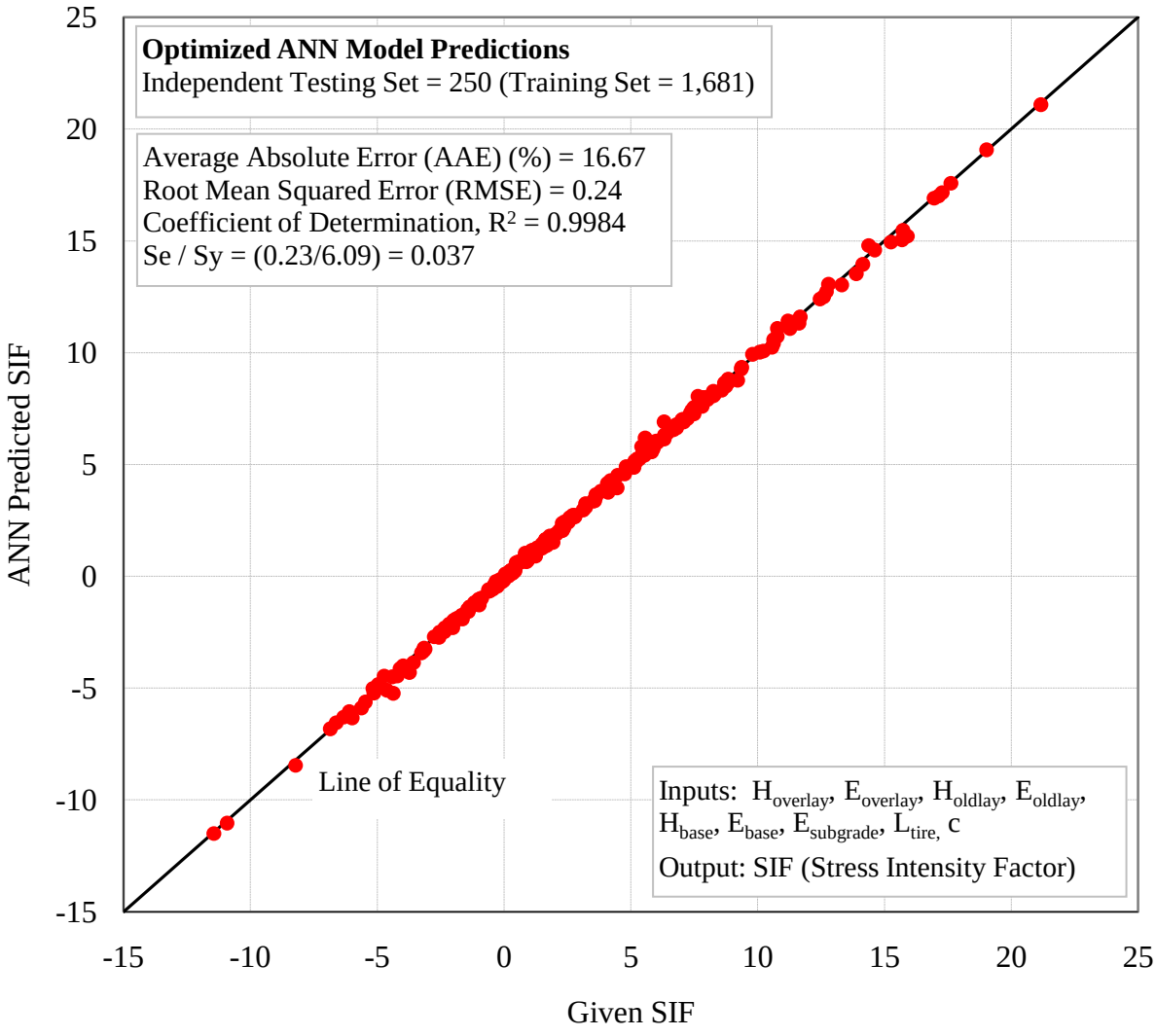

Figure F-28. ANN model of the positive and negative parts of the bending stress intensity factors for asphalt overlays over cracked asphalt surface layer (single axle–dual tire).

11. HMA Overlay on Jointed Concrete Pavement (Single Axle – Single Tire)

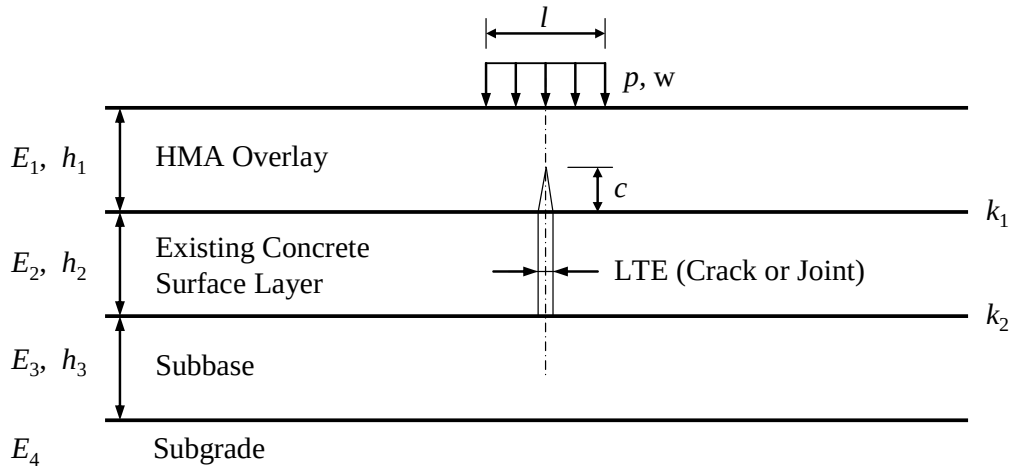

Figure F-29. Diagram of HMA overlay on jointed concrete pavement-bending.

Table F-11. Bending stress variables in HMA overlay on jointed concrete pavement system.

Variable		Unit	Value
Overlay Layer	Thickness (h_1)	mm	38, 75, 150
	Modulus (E_1)	MPa	1,000, 10,000
Interface Condition (k_1)		-	1.0
Existing Surface	Thickness (h_2)	mm	200, 300, 350
	Modulus (E_2)	MPa	20,000, 40,000
Interface Condition (k_2)		-	0.5
Subbase	Thickness (h_3)	mm	150, 600
	Modulus (E_3)	MPa	100, 1,000
Subgrade	Modulus (E_4)	MPa	30, 150
Traffic Load	Length of Tire Patch (l)	mm	64, 305, 406
	Tire Pressure (p)	psi	96
	Tire Width (w)	mm	200
Load Transfer Efficiency (LTE)		-	0.3, 0.7, 1.0
Ratio of Crack Length to Layer Thickness (c / h_1)		-	0.1, 0.3, 0.5, 0.7, 0.9

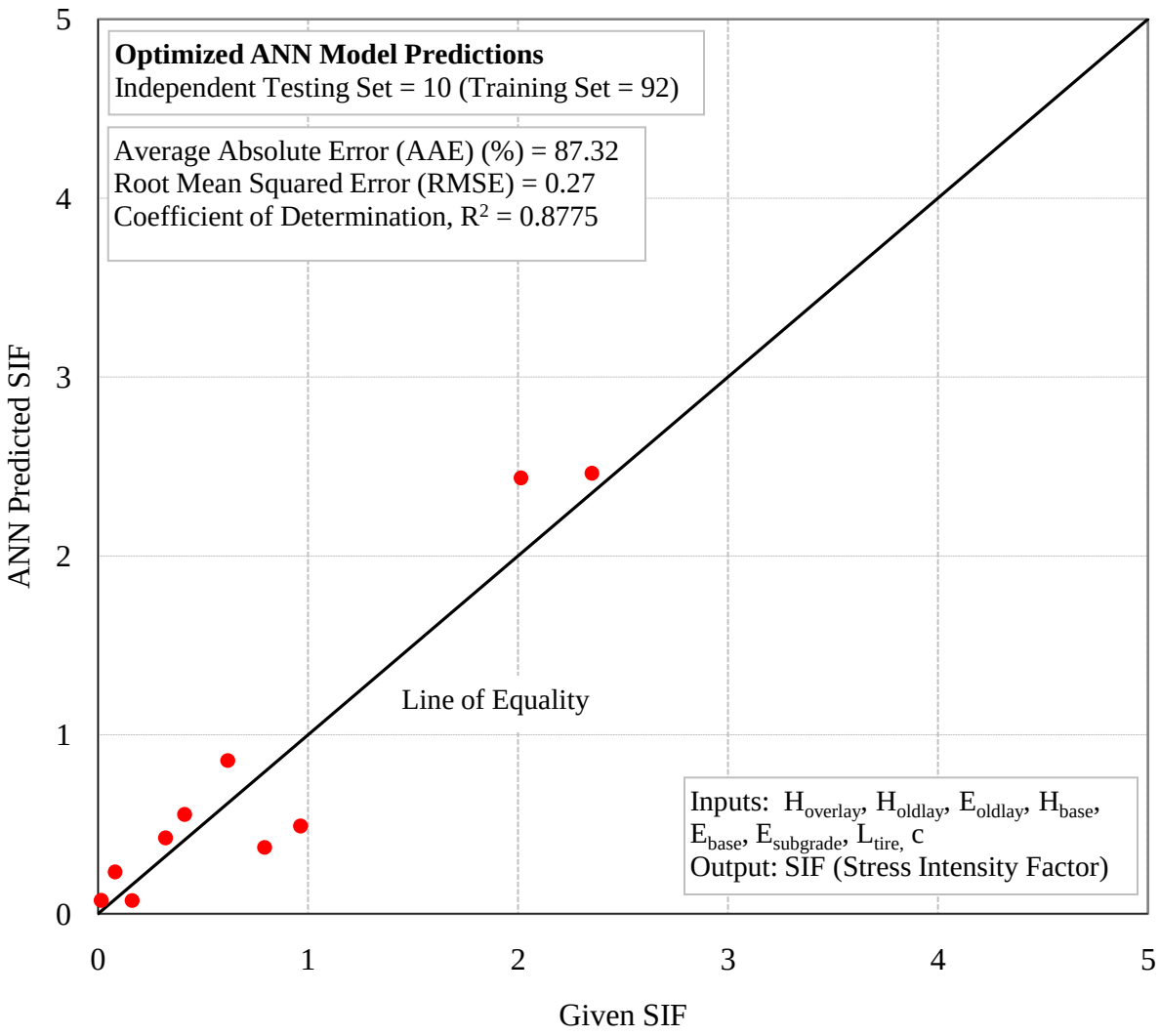

Figure F-30. ANN model of positive part of the bending stress intensity factors for asphalt overlays over jointed concrete surface layer (single axle–single tire).

As is seen in Figure F-30, there is more scatter and fewer points than with any of the other models. This is because there were so few positive bending stress intensity factors when an asphalt overlay is placed over a jointed concrete pavement. As a matter of possible interest, Figure F-31 shows the ANN model for both positive and negative Stress Intensity Factors for single axle, single tires on asphalt overlays over jointed concrete pavements. The positive model only was used in the reflection cracking program.

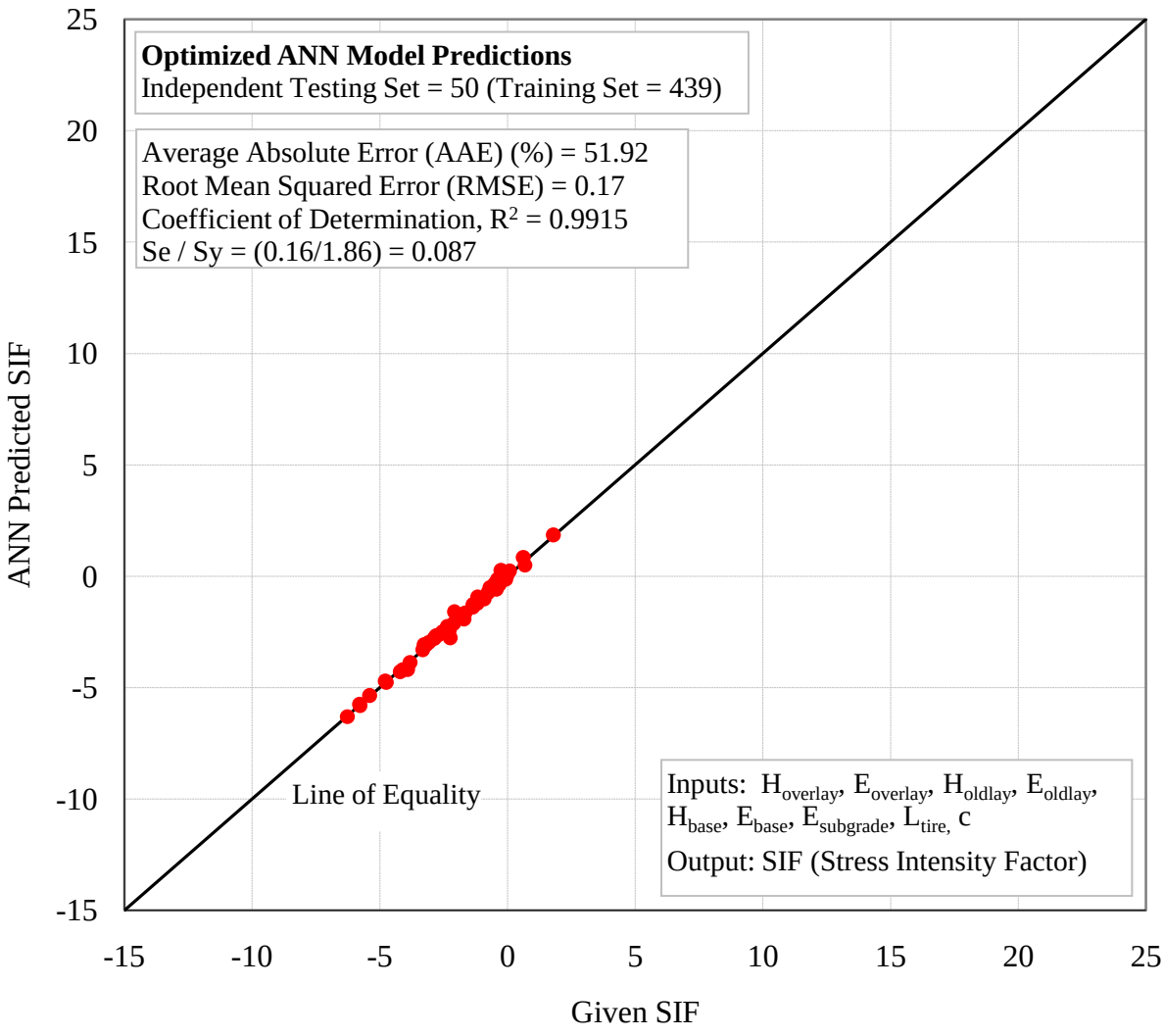

Figure F-31. ANN model of positive and negative parts of the bending stress intensity factors for asphalt overlays over jointed concrete surface layer (single axle–single tire).

12. HMA Overlay on Jointed Concrete Pavement (Single Axle – Dual Tires)

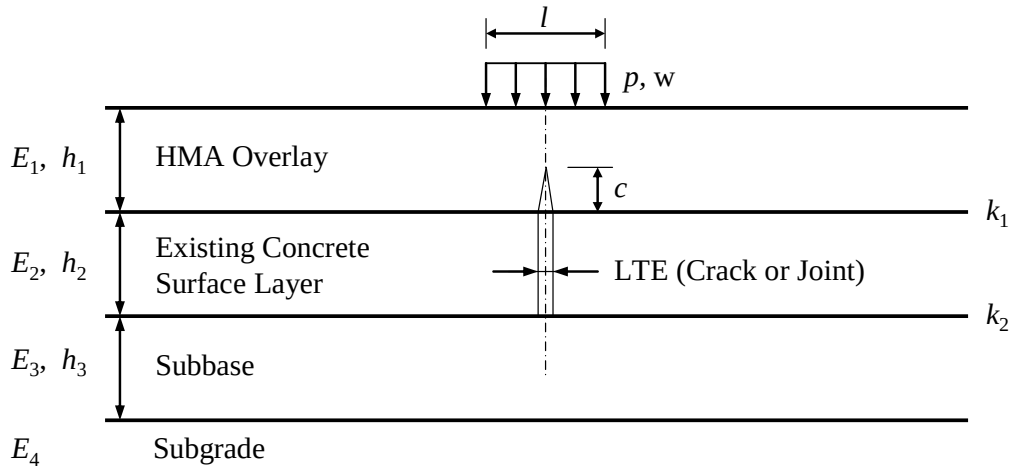

Figure F-32. Diagram of HMA overlay on jointed concrete pavement-bending.

Table F-12. Bending stress variables in HMA overlay on jointed concrete pavement system.

Variables		Unit	Value
Overlay Layer	Thickness (h_1)	mm	38, 75, 150
	Modulus (E_1)	MPa	1,000, 10,000
Interface Condition (k_1)		-	1.0
Existing Surface	Thickness (h_2)	mm	200, 300, 350
	Modulus (E_2)	MPa	20,000, 40,000
Interface Condition (k_2)		-	0.5
Subbase	Thickness (h_3)	mm	150, 600
	Modulus (E_3)	MPa	100, 1,000
Subgrade	Modulus (E_4)	MPa	30, 150
Traffic Load	Length of Tire Patch (l)	mm	64, 127, 229
	Tire Pressure (p)	psi	96
	Tire Width (w)	mm	222
Load Transfer Efficiency (LTE)		-	0.3, 0.7, 1.0
Ratio of Crack Length to Layer Thickness (c / h_1)		-	0.1, 0.3, 0.5, 0.7, 0.9

Although numerous runs were made with this dual tire case of an asphalt overlay over jointed concrete pavement, the number of positive stress intensity factors caused by bending were even fewer than in the case of the single tires. As a consequence of this, the decision was reached not to develop an ANN model of this case.